GENERATING AND MANIPULATING QUANTIZED VORTICES IN HIGHLY OBLATE BOSE-EINSTEIN CONDENSATES

by

Edward Carlo Copon Samson

A Dissertation Submitted to the Faculty of the

COLLEGE OF OPTICAL SCIENCES

In Partial Fulfillment of the Requirements
For the Degree of

DOCTOR OF PHILOSOPHY

In the Graduate College

THE UNIVERSITY OF ARIZONA

2012

THE UNIVERSITY OF ARIZONA
GRADUATE COLLEGE

As members of the Dissertation Committee, we certify that we have read the dissertation prepared by Edward Carlo Copon Samson
entitled Generating and Manipulating Quantized Vortices in Highly Oblate Bose-Einstein Condensates
and recommend that it be accepted as fulfilling the dissertation requirement for the Degree of Doctor of Philosophy

_____Date: 04/19/12
Brian P. Anderson

_____Date: 04/19/12
Poul Jessen

_____Date: 04/19/12
Ewan Wright

Final approval and acceptance of this dissertation is contingent upon the candidate's submission of the final copies of the dissertation to the Graduate College.
I hereby certify that I have read this dissertation prepared under my direction and recommend that it be accepted as fulfilling the dissertation requirement.

_____Date: 04/19/12
Dissertation Director: Brian P. Anderson

STATEMENT BY AUTHOR

This dissertation has been submitted in partial fulfillment of requirements for an advanced degree at the University of Arizona and is deposited in the University Library to be made available to borrowers under rules of the Library.

Brief quotations from this dissertation are allowable without special permission, provided that accurate acknowledgement of source is made. Requests for permission for extended quotation from or reproduction of this manuscript in whole or in part may be granted by the head of the major department or the Dean of the Graduate college when in his or her judgment the proposed use of the material is in the interests of scholarship. In all other instances, however, permission must be obtained from the author.

SIGNED: Edward Carlo Copon Samson

ACKNOWLEDGEMENTS

Foremost in my gratitudes list is my advisor, Brian P. Anderson. Without him, the experiments in this dissertation would not have been possible. I understand that coming up with experiments that are worthwhile to investigate can be challenging, but the cool experiments that you have asked me to do were really amazing, and it was a good and fun learning experience. I would like to thank him for his patience and understanding in the entire duration of my stay in his laboratory as his advisee, especially during the dissertation process. He has always been supportive of his students. I am very grateful to him for providing a very welcoming environment to a foreign student.

The experiments in this dissertation could not also have been possible without the endeavor of previous graduate students in the University of Arizona's BEC laboratory, who have built the equipments in the BEC experiment setup. Most especially, I would like to thank Tyler Neely for being a second "mentor" to me. He taught me how to operate and debug the BEC setup; he also refreshed my memory on how to design, build, and debug electronic circuits. Most of the experimental skills that I needed for this dissertation, I owe it to him. And of course, I thank him for the daily dose of jazz and funk in the experiment area, which lightened up some of the tedious days in the lab.

I would also like to thank Kali Wilson and Zachary Newman, the current graduate students in the BEC lab, both of whom I had the pleasure to work with everyday. They have helped me keep the experiments running on the times I am not in the lab, and in building some of the electronics and optical systems that were used in this dissertation. Zac also provided the numerical simulations that were used in Chapter 5 of this dissertation. I would also like to thank Kevin Gudenkauf for designing and building the amplifier circuit that were used for the PZTs in the experiment in Chapter 6.

Next, I thank the other members of my dissertation committee: Poul Jessen and Ewan Wright. Their questions, suggestions, and comments on my dissertation have been really helpful.

Thanks also to my former research advisors in the National Institute of Physics in the University of the Philippines: Caesar Saloma and Carlo Mar Blanca. They were my first research mentors, and I owe it to them for teaching me the basic research skills, dedication to the scientific endeavor, and patience and perseverance in experimentation. *Salamat po*.

I would also like to thank Jacq Romero, Athena Paz, Gay Jane Perez, and Shiela Marcos, for their friendship. I thank them for keeping me sane throughout college and grad school, especially during my last year as a PhD student.

Lastly, I would like to thank my parents, my sister, and my four aunts in Australia, for their love and support towards everything that I do.

DEDICATION

To Nanay and Daddy

TABLE OF CONTENTS

TABLE OF CONTENTS - *Continued*

TABLE OF FIGURES

ABSTRACT

This dissertation presents several experimental methods that were devised to generate or manipulate quantized vortices in highly oblate dilute-gas Bose-Einstein condensates (BECs). Studies that involve single vortex dynamics, vortex-vortex interactions, and vortex-impurity interactions are essential in developing a deeper understanding of the nature of superfluidity and in particular, superfluid turbulence. In highly oblate systems, vortex dynamics have a two-dimensional (2D) nature and the resulting superfluid characteristics may be substantially different from those in three-dimensional (3D) superfluids. However, there have been remarkably few experimental studies of 2D vortex dynamics in superfluids. Therefore, to study 2D vortex dynamics and interactions, it is necessary to first develop experimental methods that can generate vortices and vortex distributions in nominally 2D systems, such as highly oblate BECs. Four main experiments are discussed in this dissertation. Two of these experiments generate multiple singly quantized vortices in a relatively stochastic manner leading to disordered vortex distributions. From these two vortex methods, the physics of high vorticity and highly disordered systems may be observed and studied in a highly oblate system. These methods may prove useful in studies of 2D quantum turbulence. The other two experiments involve newly developed techniques for controlled generation and manipulation of vortices. One of these methods creates multiply quantized pinned vortices with a control in the generated vorticity. The other method reliably creates a pair of singly quantized vortices of opposite circulation,

whose positions can be easily manipulated after creation, such that they can be placed in any location within the BEC. The two techniques may be scalable to higher number of vortices and may prove useful in superfluid dynamics and vortex interactions that require repeatable vortex distributions. Taken together, these tools and methods may be applicable to many further studies of vortex physics in highly oblate BECs.

CHAPTER 1

INTRODUCTION

The experimental realization of Bose-Einstein condensation (BEC) in dilute atomic gases [1-3] has allowed the investigation of several quantum phenomena in a quantifiable and experimentally accessible manner. In particular, numerous experiments since 1999 have involved the formation and behavior of quantized vortices in atomic BECs, as summarized in Ref. [4]. These experiments have involved the study of vortices in numerous contexts, including quantum state manipulation, rotating BECs, phase transition dynamics, turbulence, and vortex dipole dynamics. However, only a handful of experiments [5-11] have involved the physics of vortices in nominally two-dimensional (2D) or highly oblate BECs. It is then necessary and important to have experimental capabilities in studying quantized vortices in nominally 2D dilute-gas BECs.

In a recent theoretical work [12], it was suggested that vortex dynamics and interactions can enter a two-dimensional regime, wherein the Kelvin wave vortex excitations brought about by the three-dimensional geometry of the BEC are suppressed by flattening the system. Due to Kelvin waves, which appear as tilting, wobbling, or bending of the vortex filament [13-15], energy may be dissipated, and vortices can reconnect and undergo complex dynamics in 3D. Because of the suppression of Kelvin waves, vortex interactions and dynamics in 2D systems are expected to be different from previous BEC ex-

periments, in which the 3D nature of the BEC allows for such vortex excitations. In an experiment that involved a highly oblate system [10], the observed lifetime (~2.25 s) of vortex dipoles are longer than expected from vortices of opposite circulation in a 3D system; a numerical simulation of this experiment in a spherical BEC [12] showed vortex dipoles decaying after ~100 ms. It was shown that the observation of long vortex dipole lifetimes can be attributed to the highly oblate geometry of the system and the suppression of 3D geometry-related interactions [12].

In light of these, it would be of interest to explore this regime of 2D vortex dynamics and study the different phenomena and behavior that may arise due to the suppression of Kelvin waves, treating the vortices as points in a plane. It would be especially interesting to study 2D quantum turbulence (2DQT) in these systems, and the basic vortex interactions and dynamics that may be relevant in quantum turbulence. There have been numerous theoretical work about 2DQT, but it was only recently that experimental capabilities of studying 2DQT was demonstrated; this is primarily due to the difficulty of achieving two-dimensional confinement of superfluids in experiments.

As most of the vortex creation experiments were done outside the 2D vortex dynamics regime, and in order to have a methodical and systematic way of studying this regime, it will be important to develop experimental methods that can generate quantized vortices in highly oblate geometries. The purpose of this dissertation is to present novel methods that were newly developed to create and manipulate vortices in a highly oblate trap: from generating vortex configurations with high disorder to repeatable and deterministic creation and manipulation of single vortices.

1.1 Overview of the dissertation

The second chapter discusses the general details of the experimental apparatus that was used to create, manipulate, and observe the BECs and quantized vortices in our experiments. Specific experimental steps that were used to implement the different vortex generation methods will be presented in the pertinent chapters. A brief discussion of previously reported vortex experiments that were done in the highly oblate trap geometry in our laboratory and in which the author participated will also be given in this chapter. These include the vortex dipole experiment [10], sinusoidal modulation of the radial magnetic trap [16], and the experimental observation of 2D quantum turbulence and its decay [11].

Chapter 3 presents an investigation of the rotating trap method that was used in previous BEC experiments (which produced vortex lattices), but implemented here in a highly oblate trap. Results of different rotation parameters are presented, and the evolution of vortices from their nucleation to their migration towards the BEC center will be described.

Chapter 4 describes an experiment wherein the strength of a weak repulsive potential was sinusoidally modulated in time. Effects of the modulation strength, potential location, and potential geometry to vortex generation will be discussed.

Chapters 5 and 6 present experimental methods that were developed to create vortices in a relatively controlled and deterministic manner. Chapter 5 discusses a novel method of generating pinned multiply quantized vortices in a BEC. On the other hand, Chapter 6 describes a new technique that can reliably generate singly quantized vortices and manipulate their position within the condensate afterwards.

Finally, the last chapter gives highlights of the results of the different experiments and other concluding remarks.

1.2 Quantized vortices and BECs

The study of quantized vortices provides invaluable understanding of the problem of fluid dynamics in superfluids and BECs. Unlike classical vortices that can take any value of circulation, fluid circulation in a BEC is quantized. Let us consider the macroscopic condensate wavefunction:

$$\psi\left(\vec{r},t\right)=\sqrt{n\left(\vec{r},t\right)}e^{i\phi\left(\vec{r},t\right)} \tag{1.1}$$

where $n\left(\vec{r},t\right)$ is the fluid density and $\phi\left(\vec{r},t\right)$ is a macroscopic phase [17, 18]. For this wavefunction to remain single-valued, the change in phase around any closed contour line C must be an integer q multiple of 2π i.e.

$$\int_C \vec{\nabla}\phi\cdot d\vec{l}=2\pi q \tag{1.2}$$

The velocity of a superfluid flow [17] is given by

$$\vec{v}\left(\vec{r},t\right)=\frac{\hbar}{m}\vec{\nabla}\phi\left(\vec{r},t\right) \tag{1.3}$$

where m is the mass of an atom in the fluid. From eqs. (1.2) and (1.3), it implies that the circulation around any given point is

$$\int_C \vec{v}\cdot d\vec{l}=q\left(\frac{h}{m}\right) \tag{1.4}$$

i.e. the circulation of fluid in a BEC is quantized in units of h/m. Equivalently, a phase-winding of 2π in the condensate phase defines the presence of a singly quantized vortex.

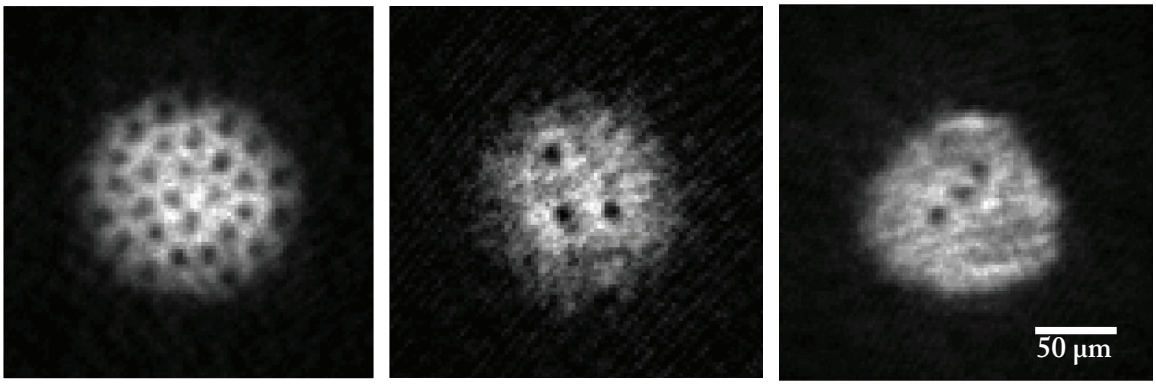

Figure 1.1 Typical absorption images of expanded BECs that contain vortices. The vortex cores can be resolved after expansion of the BEC and are represented as circular holes in the condensate density.

At the center of this phase-winding, the phase is undefined, and as we approach this discontinuity in phase, the fluid velocity [as defined in eq. (1.3)] diverges. Because the system has finite energy, the condensate density decreases to zero at the phase discontinuity [19]. This zero density defines the central axis of the core of the quantized vortex. The core size is defined by the coherence or healing length ξ of the condensate, given by

$$\xi = \frac{1}{\sqrt{8\pi an}} \tag{1.5}$$

where a is the s-wave scattering length and n is taken as the bulk value of the density [17]. Through this absence of density in the core, imaging of vortices are possible by observing circular gaps in the condensate density. A typical image of a condensate having vortices is shown in Figure 1.1.

1.3 Gross-Pitaevskii equation (GPE)

At a very low temperature $T \ll T_C$ (where T_C is the BEC transition temperature) and for a large number of condensate atoms, thermal and quantum effects are minimal, and atomic BEC can be approximateed by a mean-field macroscopic wave function, as defined in eq. (1.1) [17]. The dynamics of this wavefunction are well-described by the Gross-Pitaevskii equation (GPE) ,

$$i\hbar\frac{\partial\psi\left(\vec{r},t\right)}{\partial t}=\left[-\frac{\hbar^2}{2m}\nabla^2+V_{ext}\left(\vec{r},t\right)+g\left|\psi\left(\vec{r},t\right)\right|^2\right]\psi\left(\vec{r},t\right) \tag{1.6}$$

where V_{ext} is the external confinement and m is the atomic mass. The nonlinear coefficient $g = 4\pi\hbar^2 a/m$ governs the atomic interactions. The nonlinear term originates from particle-particle interactions and is a good approximation for dilute systems or systems with weak interactions between particles.

Since this dissertation will discuss experiments in highly oblate BECs, bending and Kelvin wave excitations of the vortex lines are inhibited, and a 2D description of the dynamics will be sufficient. For this condition, it is adequate to use the computationally advantageous two-dimensional GPE (2D GPE) for numerical simulations in the x-y plane. The numerical simulations that were used in chapters 5 and 6 involved 2D GPE methods.

CHAPTER 2

THE BEC EXPERIMENT SETUP

This chapter provides the details of the Bose-Einstein condensation apparatus that was used for all of the experiments in this dissertation. The main BEC apparatus was primarily constructed by two former graduate students of the BEC laboratory, David Scherer and Chad Weiler. A more detailed discussion of the apparatus can be found in their dissertations [20, 21]. The optical setup that facilitated the conversion of our time-averaged orbiting potential (TOP) trap [22] into a highly oblate optical and magnetic trap was built mostly by another former graduate student, Tyler Neely. An extensive discussion of this setup is found in his dissertation [16]. Only a short description of the BEC apparatus is given here.

2.1 Initial cooling with the magneto-optic trap (MOT)

The main BEC apparatus is a two-chamber ultra-high vacuum system, with a single magneto-optical trap (MOT). A set of SAES ^{87}Rb dispensers provides low-pressure ^{87}Rb gas to the system. These dispensers are located at the back end of the MOT cell. The apparatus achieves a pressure of ~ 10^{-9} Torr in the MOT cell (with a dispenser on), whereas lower pressures of ~ 10^{-12} are in the cell where BECs are formed. These cells are shown in a photo of the apparatus in Figure 2.1.

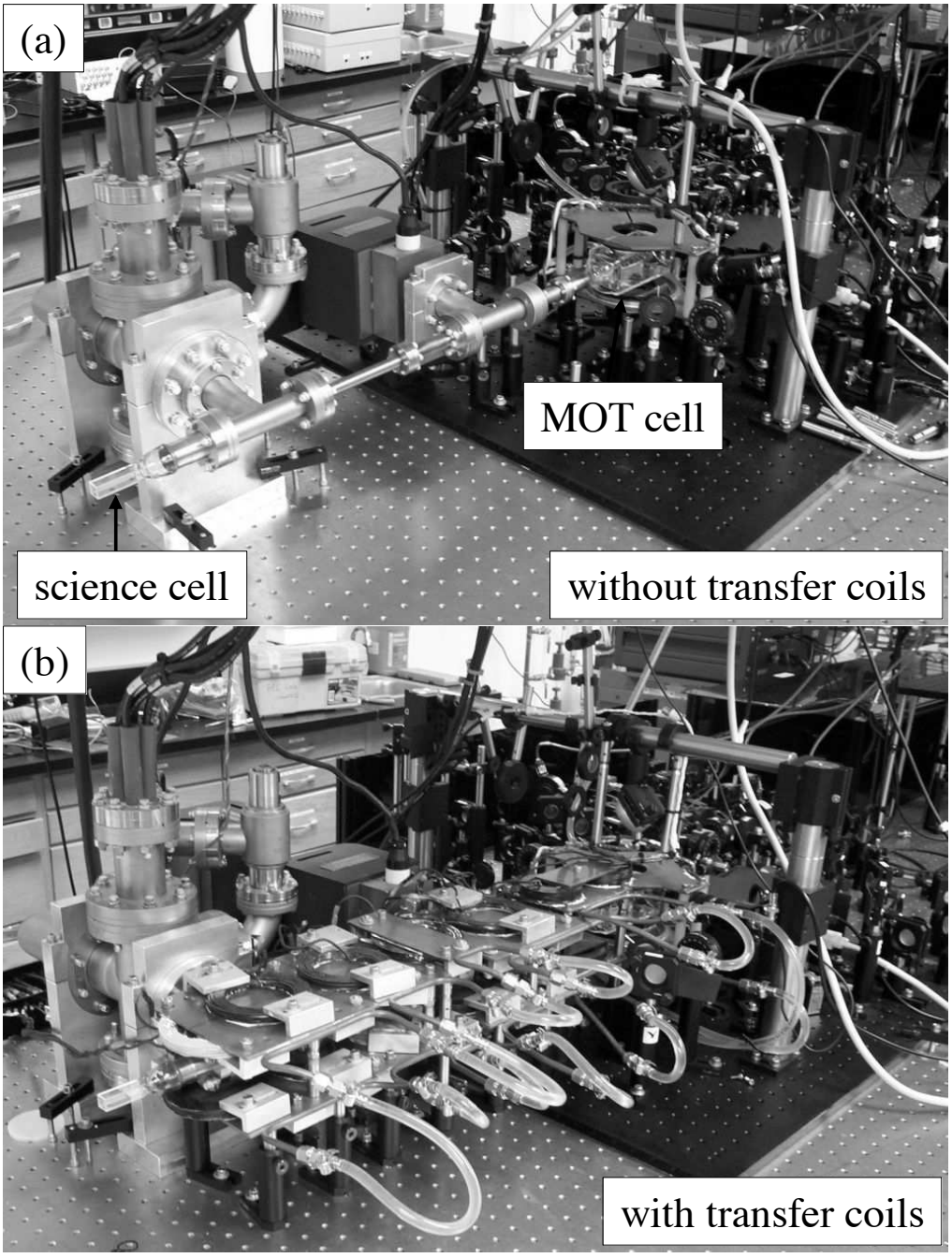

Figure 2.1 (a) Picture of the two-chamber vacuum system. The MOT cell is in the far end of the tube, while the BEC science cell is in the foreground. (b) The vacuum system with the magnetic transfer coils placed in position. This figure was taken from Ref. [20].

The first stage in creating BECs in this apparatus involves laser cooling of the ^{87}Rb atoms in the MOT cell. To form the magneto-optic trap, near resonant 780-nm laser light is split into six beams, with each of the beams being directed toward the MOT cell. The power of the original beam is ~ 500 mW. The six beams are divergent as they approach the cell, with ~ 2 in. diameters at the MOT center. These six beams form three pairs of counter-propagating beams with one pair for each orthogonal spatial axis. This laser light is red-detuned from the resonant wavelength for the $|5\ ^2S_{1/2},\ F = 2\rangle \longrightarrow |5\ ^2P_{3/2},\ F' = 3\rangle$ transition in ^{87}Rb by 4.5Γ, where $\Gamma = 2\pi \times 5.9$ MHz is the natural linewidth of the ^{87}Rb transition. Because of this, atoms that are moving against the direction of propagation of the beam will see this light Doppler-shifted into resonance; hence, these atoms will preferentially scatter light from beams opposing their motion and lose kinetic energy in the process [23]. To complete the MOT, there is an 8 G/cm axial spherical quadrupole magnetic field. A repump beam tuned near the $|F = 1\rangle \longrightarrow |F' = 2\rangle$ transition is also necessary. This beam has a total power of ~ 30 mW and is split into four beams and directed to two orthogonal directions of the MOT cell. The resulting MOT has ~ 3×10^9 atoms with an approximate temperature in the order of tens of μK.

2.2 Magnetic transfer to a TOP trap

When the atom cloud in the MOT has reached a certain size threshold, the next sequence in the BEC formation process involves the transfer of the atom cloud into the BEC science cell. The atoms undergo an initial compressed MOT (CMOT) stage [22] for a duration of 60 ms. At this stage, the MOT is spatially compressed, causing a tem-

porary increase in its density. This process involves the sudden increase in detuning of the cooling beams to around -9Γ, a reduction in the repump beam light intensity to ~10% of its initial value, and a linear decrease of the quadrupole field from 8 G/cm to 0 G/cm. Due to this process, the atoms in the MOT are optically pumped to the $|F = 1, m_F\rangle$ states. Afterwards, the atoms are loaded in a quadrupole magnetic field with an axial gradient of 160 G/cm. This process traps the atoms projected into the $|F = 1, m_F = -1\rangle$ state. After the CMOT stage, the atoms in the MOT are transferred to the BEC cell by sequentially turning on and off a series of magnetic coil pairs (see Figure 2.1b). A detailed description of the mechanism for this transfer sequence can be found in Ref. [20].

At the BEC cell, the atoms equilibrate in the axial gradient field of 160 G/cm for 1 s. Afterwards, the field gradient value jumps to 266 G/cm. An additional magnetic bias field of 43 G is then added. The bias field points in the horizontal plane and its direction is rotated along the plane with an angular frequency of $\omega_{rot} = 2\pi \times 4$ kHz. This has the effect of pushing out the zero point of the quadrupole field in a circular orbit. This trap configuration is the time-averaged orbiting potential (TOP) trap. The resulting TOP trap has a time-averaged harmonic radial trapping frequency of $\omega_r = 2\pi \times 40$ Hz.

2.3 Transfer to a highly oblate trap and evaporative cooling

The next process in BEC formation involves linearly decreasing the magnetic bias field to 5 G, with a simultaneous radio-frequency (rf) induced evaporation for 60 s. This further cools the atoms. The axial gradient field is then decreased from 160 G/cm to 52 G/cm; this causes the center-of-mass position of the cloud to sag due to gravity by 0.56

mm. The resulting TOP trap is weaker with a radial trapping frequency of $\omega_r = 2\pi \times 7.8$ Hz.

With the TOP trap still present, the atoms are then loaded to a into a red-detuned laser light sheet. This is accomplished by linearly increasing the power of a 1090-nm beam to ~ 1 W for a duration that was variable in our different experiments (ranged from 2.5 to 4.0 s). This red-detuned beam is precisely aligned at the center-of-mass position of the atoms in the weak TOP trap to facilitate efficient loading. The red-detuned light sheet squeezes the atom cloud along the axial direction. This causes our combined magnetic and optical trap to have a highly oblate geometry. A discussion of the details of the red-detuned light sheet used in this experiment can be found in Ref. [16]. Once the atoms are loaded into the combined magnetic and optical trap, a final stage of rf-induced cooling is used to form a highly oblate BEC. The resulting trap has a radial trap frequency of $2\pi \times 8.0$ Hz, and an axial trap frequency of $2\pi \times 90$ Hz. This gives our trap an aspect ratio of R_z:R_r = 11:1. BECs formed in this trap typically contain 2×10^6 atoms with a temperature $T \sim 52$ nK. A recent numerical study of our trap has confirmed that with this aspect ratio, it is in the regime of two-dimensional vortex dynamics [12]. It should be noted though that despite being in the regime of 2D vortex dynamics, the BEC chemical potential is $\mu_0 \sim 8\hbar\omega_z$, where ω_z is the axial trapping frequency. This makes our BEC in itself three-dimensional in nature [19, 24]. Representative images of the BEC formed in this trap are found in Figure 2.2.

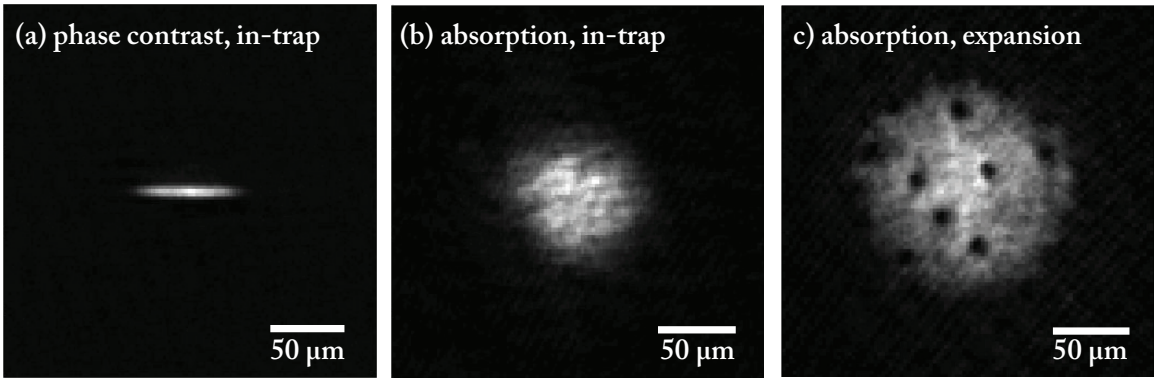

Figure 2.2 Representative images of the BEC taken by the imaging system in our experiment setup. (a) Phase-contrast image of an in-trap BEC, taken along the horizontal imaging axis. Absorption images of (b) an in-trap and (c) expanded BEC, taken along the vertical imaging axis.

2.4 Imaging systems

There are two imaging modes that are used in our experiments. Phase contrast imaging is typically used along the horizontal axis of our system (see Figure 2.3). It is normally utilized to take in-trap images of the BEC. Absorption imaging is typically used along the vertical axis of our system, and is utilized to take images of both in-trap and expanded conditions of the BEC.

2.4.1 Phase contrast imaging

Phase contrast imaging is accomplished through the use of detuned light, that is typically red-detuned from the $|F = 1\rangle \longrightarrow |F' = 2\rangle$ transition. A typical value of the detuning is 900 MHz. The detuned light passes through a 100 μm × 100 μm phase dot at an intermediate focal plane (see Figure 2.3). The phase dot adds a $3\pi/2$ phase shift in the detuned light. In this intermediate focal plane, the light scattered by the BEC is not fo-

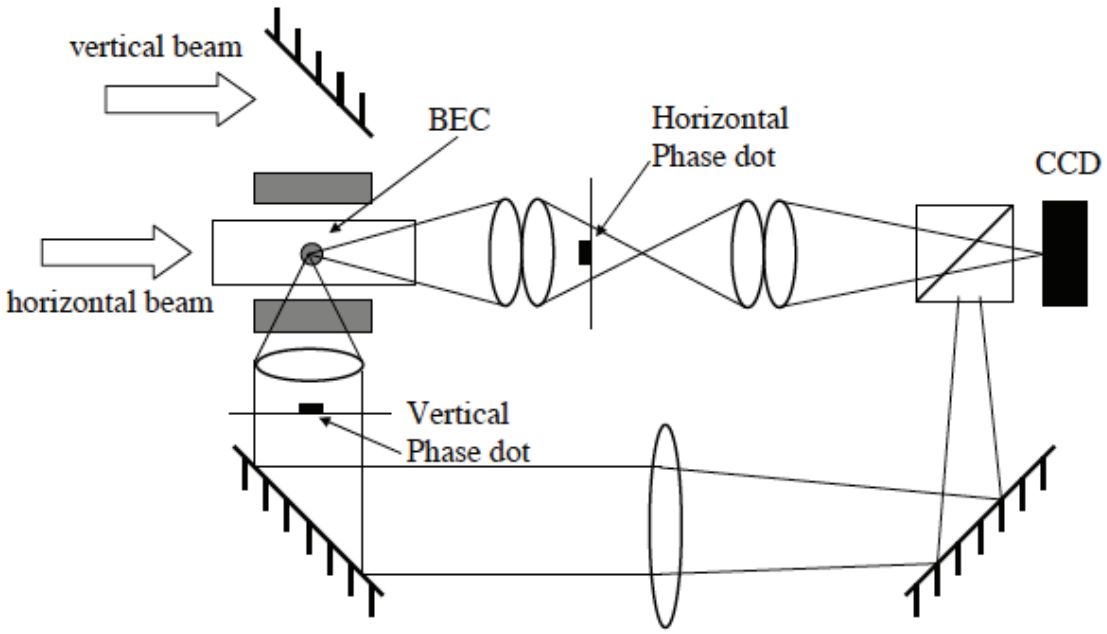

Figure 2.3 Schematic diagram of the two imaging axes in our experimental setup. The horizontal imaging axis is primarily used to take in-trap phase contrast images, while the vertical imaging axis is typically used for absorption images (with the vertical phase dot removed). This image was taken from Ref. [20].

cused; hence, it is negligibly affected by the phase dot. At the image plane of the CCD imaging device, the phase-shifted background light and the unshifted BEC light scatter undergo interference to produce an image. The resulting image has a dark background with a bright image of the BEC. A phase contrast image of the BEC along the horizontal imaging axis is shown in Figure 2.2a.

2.4.2 Absorption imaging

Absorption imaging uses laser light tuned closely to the $|F = 2\rangle \longrightarrow |F' = 3\rangle$ transition. The light is collimated and directed through the BEC cell. Absorption imaging is typically used along the vertical axis; hence, the imaging light is incident on the top

of the BEC cell. The trapped BEC atoms are in the $|F = 1, m_F = -1\rangle$ ground state so it is not accessible to the imaging light. Therefore, a pulse of optically pumping light is used to pump the atoms to the $|5\ ^2S_{1/2}, F = 2\rangle$ level. After this pumping pulse, a pulse of the absorption imaging light is directed at the BEC. Scattered light from the BEC reaches the image plane of the CCD imaging device, wherein a shadow of the BEC is recorded. The resulting image has white background, with the a dark BEC. This image undergoes post-processing to render the BEC in white, while the background goes dark. A typical absorption image of an in-trap BEC is shown in Figure 2.2b.

The healing length of the BEC in our system is ~ 0.3 μm, which is below the imaging resolution of our system (~3.4 μm). Because of this, vortex cores cannot be resolved by our imaging system when the BEC is in the trap. In order to image the vortex cores, expansion of the BEC is necessary. Expansion is accomplished by first turning off the rotating radial bias field and applying an extra expansion field with a gradient along the axial direction. This produces a total axial field gradient of ~ 32 G/cm. The red-detuned light sheet is kept on, which allows the BEC to expand only in the radial direction. After 10 ms, the 1090-nm light is snapped off and the cloud expands for an additional 35 ms. The normal absorption imaging sequence then follows. A typical representative absorption image of an expanded BEC along the vertical axis is shown in Figure 2.2c. The vortex cores are seen here as circular holes in the expanded BEC.

2.5 Previous experiments in highly oblate BECs

This section provides a brief summary of experiments that were conducted in the highly oblate trap in our laboratory, in which the author has participated. All of these

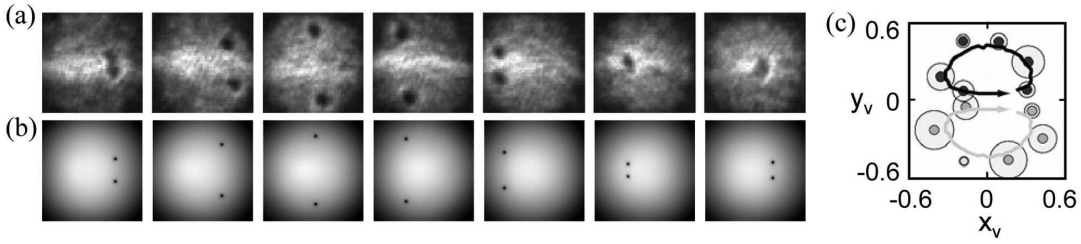

Figure 2.4 Sequence of images showing the first orbit of vortex dipole dynamics. (a) Consecutive images showing the dipole orbit for a single dipole, with 200 ms between successive images of the expanded BEC. (b) Corresponding images of the BEC from numerical simulations performed under similar conditions, with $T = 0$. (c) Average positions of the two vortices from 5 sequences of experimental data. The circle around each position indicates the standard deviation of the vortex position. This set of images was taken from Ref. [16].

experiments have been reported in other references, which are suggested for a more detailed discussion. These experiments include vortex dipoles [10], symmetric sinusoidal modulation of the magnetic radial trap [16], and and the experimental observation of 2D quantum turbulence and its decay [11]. Summaries of these experiments are provided in this section in order to give a complete description of the methods that were used to study vortices in highly oblate trap in our laboratory.

2.5.1 Vortex dipole experiment

In this experiment, controlled coherent nucleation of singly quantized vortex dipoles in a highly oblate BEC was demonstrated. This involved swiping a blue-detuned potential across the condensate at a speed that is above the critical velocity to shed vortices. Observation of the dipole dynamics (as shown in Figure 2.4) became possible because of the repeatability of the vortex nucleation method. The dipole dynamics reveal the circulation direction of each vortex and showed that the dipole has relatively long life-

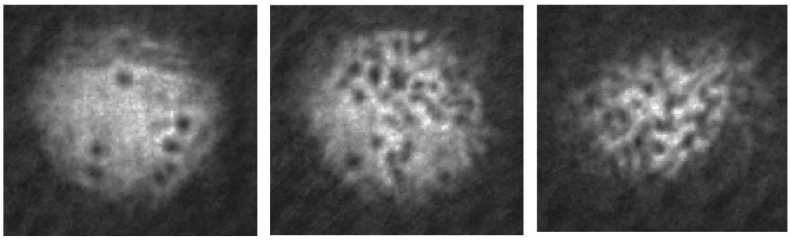

Figure 2.5 Excitation of a toroidally trapped BEC through harmonic modulation of the magnetic trapping potential. As the modulation time t_{mod} is increasing, vortices begin to appear in the system. This set of images was taken from Ref. [16].

time. Sufficiently rapid swiping of the blue-detuned potential caused vortices of identical circulation direction to aggregate into multiply charged vortex dipoles.

2.5.2 Radial trap modulation

In these experiments, the amplitude of the TOP trap's magnetic bias field was sinusoidally modulated. With increasing modulation time, vortices were observed to appear in the condensate. Because no net angular momentum was transferred into the system, it was assumed that these vortices can be of either sign of circulation. The same method was performed on the presence of a blue-detuned potential in the center of the trap (see figure 2.5). Shorter modulation times were needed to induce nucleation of vortices in this system. It also seemed that the vortices originated within the condensate, as opposed to getting nucleated from its edge. The exact mechanism of vortex nucleation in this experiment is not yet clear.

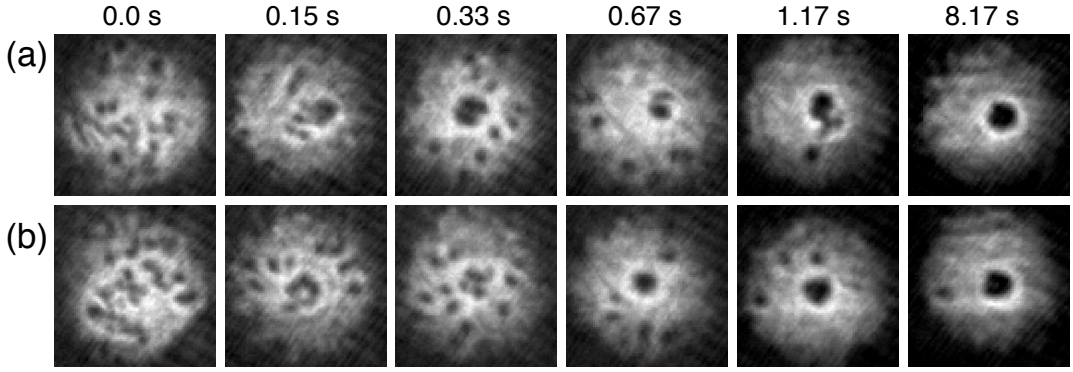

Figure 2.6 (a) and (b) Superflow formation process from a highly disordered vortex distribution. Indicated times are hold times in the trap prior to image acquisition. This set of images was taken from Ref. [11].

2.5.3 2D quantum turbulence (2DQT) generation and decay

In this experiment, a BEC was formed in the highly oblate trap with an axially propagating blue-detuned beam located at the trap center. After formation, the blue-detuned beam was then effectively translated along a small circular path (~ 5.7 μm in diameter; the BEC radius is ~100 μm) in the BEC center. This motion induces small-scale forcing and nucleation of numerous vortices in a highly disordered distribution inside the BEC, and is identified with the occurrence of 2DQT. Afterwards, the BEC remains in the annular trap, and the decay of 2DQT was observed. It was noted that the disordered vortex distribution gradually evolved into a persistent current. This evolution is shown in Figure 2.6.

CHAPTER 3

ROTATING A CONDENSATE IN A HIGHLY OBLATE TRAP

This chapter discusses experiments involving Bose-Einstein condensates that were subjected to trap rotation while held in a weakly elliptical trap with a highly oblate configuration. Beyond a critical rotation frequency, vortices were nucleated in the BEC. Their evolution during and after rotation was observed. The effects of the different rotation parameters were also investigated.

3.1 Motivation

A few of the very first experiments that were conducted after dilute gas Bose-Einstein condensates were experimentally realized were forced rotation of the trap confining the BECs, either by laser beams [25-29] or by temporal manipulation of the magnetic trap [30-32]. From these experiments, vortex nucleation and formation of vortex lattices were observed when the rotation frequency reached a particular critical value. The dynamics of vortex nucleation and the formation of vortex lattices have both been studied numerically [33-37] and experimentally [28, 29, 32]. Due to the three-dimensional geometry of these BEC experiments, the interaction of the vortices are influenced by tilting and bending of the vortex filaments. Vortex bending and tilting have been both predicted numerically [38-41] and observed in experiments [13, 14, 42].

Observation of these interactions and vortex dynamics can be limited by conventional imaging methods that compress information into two dimensions. In highly oblate systems, such as ours, vortex bending is inhibited and vortex filaments remain straight along the z-axis [41]. Therefore, vortex motion can be observed in the transverse plane without being concerned about the vortex structure along the axial direction.

Additionally, the absence of filament bending and tilting in highly oblate condensate should lead to a slightly different vortex interaction and dynamics [12]. Motion of the vortices are now constrained in only two dimensions, and a different kind of physics should be expected. In fact, Ref. [43] has proposed that turbulence confined in 2D plays a key role in vortex lattice formation. Furthermore, most numerical simulations of rotating BECs are performed in the 2D limit and using the 2D time-dependent Gross-Pitaevskii equation (2D GPE) [34, 36, 43-45].

In the context of 2D quantum turbulence, a method to generate large distributions of singly quantized vortices of the same circulation sign within a BEC should be useful. In a recent theoretical study [46], a new method to characterize 2D quantum turbulence in terms of vortex position measurements and vortex spatial separations was suggested. These measurements are experimentally feasible and can be performed using typical images of BECs that contain vortex cores. BECs that have undergone trap rotation may provide a system in which this large distribution of vortices can be observed, and experimental characterization of 2D quantum turbulence using vortex positions and distances can be performed. With this vortex generation process, it is highly likely that the vortices will have the same circulation sign, which makes characterization of vortex turbulence relatively simpler, without having to worry about the circulation direction of each

individual vortex. In light of these, an experiment that involves rotation of condensates with highly oblate geometries and observation of vortex nucleation and dynamics confined in 2D should be of interest.

This chapter is organized in this manner: the next section gives a brief description of the procedure that was used to rotate the BEC in the highly oblate trap. Section 3.3 discusses the effect of the different rotation parameters on the number of vortices that was generated in the condensate after rotation. Section 3.4 details the evolution of the condensate during and after rotation inside the trap. Lastly, the final section provides a short summary of the highlights in this chapter.

3.2 Description of experimental methods

Highly oblate Bose-Einstein condensates that were produced by the methods that were described in Chapter 2 were used in this experiment. After rf-induced evaporation has ended, the condensate was made to rotate about the vertical (z) axis of the trap, similar to procedures that were performed to create a vortex lattice in BECs, as described in Refs. [47] and [32]. This vortex lattice formation procedure have already been implemented in our laboratory in prior experiments [16, 20]. A detailed description of the hardware and procedure that were used in this experiment to rotate the BEC in the trap is described in Ref. [20].

In order to accomplish BEC rotation, the TOP trap was distorted into an elliptical geometry along the x-y plane, and was made to rotate at a particular frequency. This distortion was achieved by adding a sinusoidal signal from an external function generator

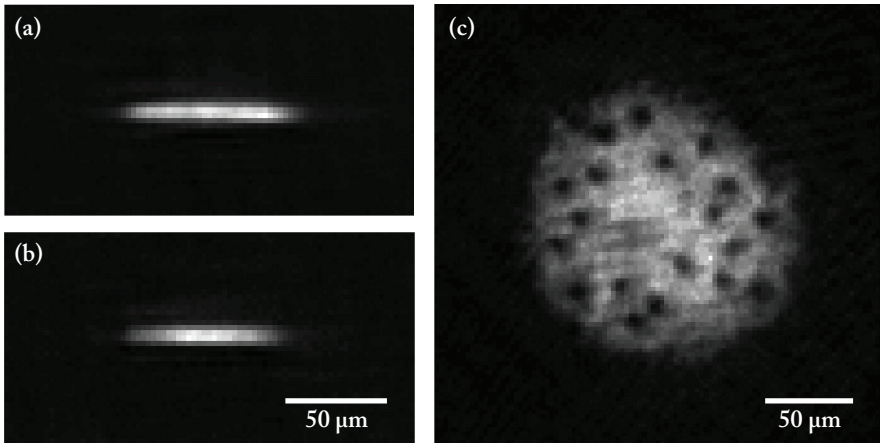

Figure 3.1 In-trap images of the highly oblate condensate along the horizontal imaging axis (a) before and (b) after rotation of the magnetic trap. As can be seen from the two images, the BEC retained its highly oblate aspect ratio even after rotation. (c) Typical vertical absorption image of the BEC after rotating the magnetic trap (while keeping the tight confinement along the z-direction) and letting the condensate expand. Quantized vortices were nucleated and were spread out across the BEC. The parameters that were used for this image are: $\nu_{spin,eff}$ = 6.0 Hz, V_{spin} = 0.017 V, t_{spin} = 1.0 s, and t_H = 2.0 s.

to the TOP trap signal. The sinusoidal signal was governed by the following parameters: a peak-to-peak amplitude V_{spin}, that governs the ellipticity of the TOP trap, and frequency ν_{spin}, which is twice the effective rotation frequency of the trap $\nu_{spin,eff}$. For clarity, the frequencies that would be reported here are the effective rotation frequency (i.e. the value that was inputted to the function generator would always be twice the values reported here). This rotation signal was applied to the trap for different time durations t_{spin}. When the trap is rotated, the RF frequency was increased to 8 MHz to prevent further loss of atoms. After a certain amount of hold time t_H after rotation, the BEC was allowed to expand, and absorption imaging followed.

Figure 3.1a-b shows in-trap phase contrast images of the BEC taken along the horizontal (x) imaging axis and presents a comparison of the highly oblate condensate

before and after rotation. As can be seen from this side-by-side comparison, the BEC maintained its highly oblate geometry while inside the trap after rotation.

3.3 Effects of rotation parameters on vortex nucleation

Figure 3.1c is a representative absorption image of an expanded condensate after rotation. The parameters that were used for this image are: $\nu_{spin,eff}$ = 6.0 Hz, V_{spin} = 0.017 V, t_{spin} = 1.0 s, and t_H = 2.0 s. As seen from the image, quantized vortices were generated in the condensate after rotation, as manifested by the presence of vortex cores. A total of 19 vortex cores can be seen in this image. Even though a lattice was not present in the image and the vortex configuration seemed disordered, we are assured that each vortex core in the image corresponds to exactly one vortex filament. Due to the highly oblate nature of the condensate, vortices should stay straight along the z axis [12, 41], and filament bending (as observed in Ref. [13]) should be inhibited in this geometry.

Figure 3.2 shows a plot of the number of visible vortex cores in the BEC when the rotation frequency was varied. In previous experiments where the condensate was rotated, and eventually led to nucleation of vortices and formation of vortex lattices [25-30, 32, 48], the rotational frequency had to be at least equal to $\sim \frac{1}{2\pi}\frac{\omega_\perp}{\sqrt{2}} \sim 0.71\frac{\omega_\perp}{2\pi}$ in order to excite the quadrupolar instability of the BEC and initiate vortex nucleation [49, 50], where $\omega_\perp$ is the transverse trapping frequency. As such, we varied the rotation frequency near the vicinity of this critical value: 3 Hz to 7 Hz in increments of 0.5 Hz, with $\omega_\perp = 2\pi \times 8$ Hz in our trap. The other parameters that were used for this part of the ex-

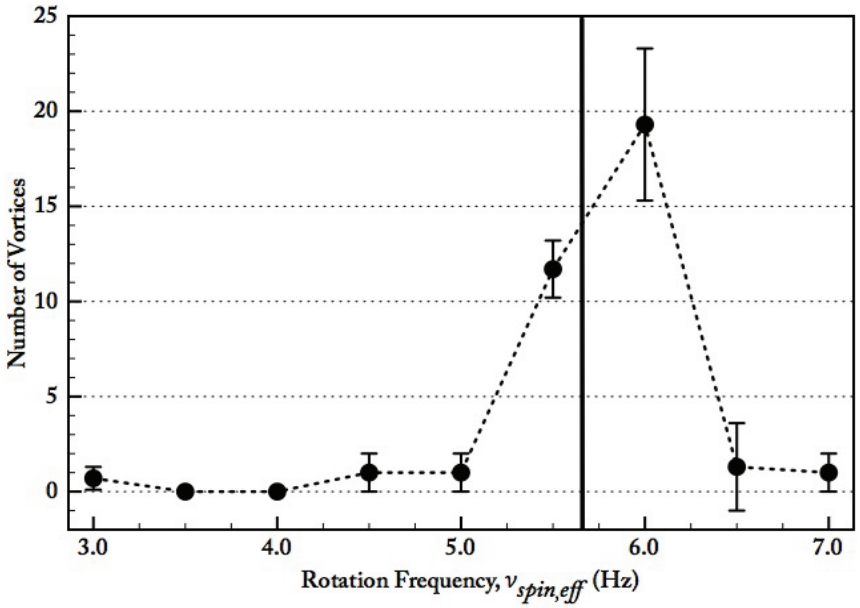

Figure 3.2 Plot of the number of vortices inside the condensate at different rotation frequencies of the magnetic trap. The highest number of vortices were observed at 6.0 Hz. This is above the critical frequency (~5.65 Hz, indicated by solid vertical line) of the harmonic magnetic trap in order to nucleate vortices. At 4.0 Hz, the BEC got very heated and disintegrated into a thermal cloud; hence, a zero value for the number of vortices observed. The other rotation parameters for this set were: V_{spin} = 0.017 V, t_{spin} = 1.0 s, and t_H = 2.0 s. The error bars indicate standard deviations of the measurements.

periment are: V_{spin} = 0.017 V, t_{spin} = 1.0 s, and t_H = 2.1 s. As can be seen from the plot, the number of vortices that were observed in the BEC was highest at a rotational frequency window of 5.5 to 6.0 Hz. This is consistent with the expected value as the critical rotation frequency is ~5.65 Hz, as indicated by a solid vertical line in Figure 3.2.

With the rotation frequency set at 6.0 Hz and V_{spin} = 0.017 V, the number of generated vortices at different spin durations were investigated. Expansion and imaging of the condensate happened after a 2.5-s hold time subsequent to rotation. As seen in Figure 3.3 (hollow circles), the number of vortices in the BEC peaked after spinning the condensate for 1 s and decreased afterwards. It is not completely known why there is a

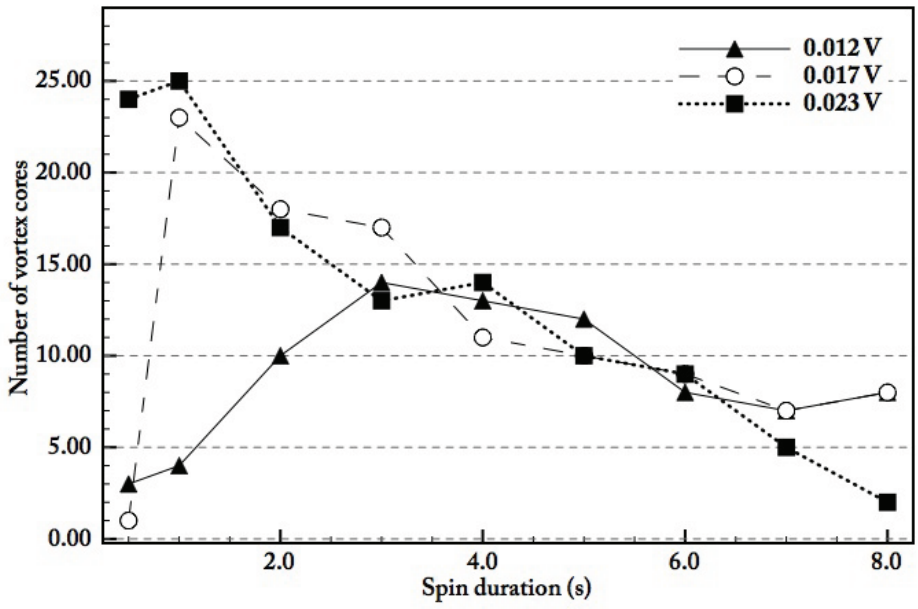

Figure 3.3 Plots of the number of vortices inside the BEC at different time durations of the spinning. Each curve corresponds to different amounts of ellipticity for the rotating magnetic trap. The indicated voltage is the peak-to-peak voltage of the sinusoidal signal from a function generator that controls the ellipticity and rotation of the trap. A higher voltage corresponds to a higher ellipticity. From the plots, it could be seen that a lower ellipticity requires a longer spin time to generate a significant number of vortices. Nevertheless, a lower ellipticity generates relatively fewer vortices. The decrease in vortices with increasing rotation time could be attributed to heating of the BEC with longer rotation and damping of vortices with longer interaction with the thermal non-condensate fraction. The rotation frequency for this data set was 6.0 Hz, and t_H = 2.5 s.

decrease in the number of vortices but we can speculate that this is due to energy dissipation as the vortices and BEC interact with the thermal background [51, 52]. The 2.5-s hold time after rotation could have allowed interaction between the vortices and the higher thermal fraction, which would lead to damping and loss of vortices in the condensate.

A smaller and larger level of ellipticity were also used for different spin durations, as can be seen in Figure 3.3. As expected, the smaller ellipticity produced a smaller number of vortices, and required a longer spin time to produce a significant amount of vorticity. This is because at lower ellipticity, the buildup of angular momentum in the BEC take place more gradually than at a higher ellipticity [36]. At a bigger ellipticity, the decrease in vortices was steeper at longer spin durations. Again, this agrees with heating of the BEC due to rotation, and with a higher ellipticity, the heating should be more pronounced.

3.4 Observing nucleation and evolution of vortices in the BEC

The process of vortex nucleation during the rotation of the Bose-Einstein condensate in the highly oblate trap and the evolution of vortices afterwards were observed in detail by obtaining axial absorption images of the BEC during and after rotation. The dynamics of vortices in this process has been studied extensively in numerical simulations [34, 36, 43-45]. Parker and Adams [43] have proposed four stages in this process: (a) fragmentation, where the quadrupolar mode of the BEC breaks down, and energetic atoms are ejected out to form an outer cloud; (b) symmetry breaking, where rotational symmetry is broken in a macroscopic manner, and allows the rotation to couple to addi-

tional modes that lead to vortex nucleation; (c) turbulence, where a turbulent state containing vortices is formed; and (d) crystallization, where the system relaxes due to loss of energy.

Shown in Figure 3.4 are absorption images of the expanded condensate at different instances during the rotation process and a few seconds after rotation. The rotation parameters for this set of images are: $\nu_{spin,eff}$ = 6.0 Hz, V_{spin} = 0.017 V, and t_{spin} = 1.0 s. It should be noted that this set of images consists of different BECs (that underwent the same procedure); due to the destructive nature of absorption imaging, it was not possible to derive a time evolution from a single BEC.

The observed evolution of the BEC has good agreement with the results of the simulations from Refs. [34, 36, 43, 45]. From the images, we can clearly see the fragmentation process, as mentioned above. The BEC underwent elongation as soon as the rotation started. Since the rotation frequency is nearly resonant with the quadrupole mode, a dynamical instability is expected [49]. This instability is manifested by the ejection of atoms from the ends of the condensate, and can be perceived as low density tails (500-ms, 700-ms, 1-s images). Eventually, vortices are seen to start nucleating at the edge of the condensate (1.0- to 1.3-s images). This is due to the breakdown of rotational symmetry as the surface of the condensate interacts with the thermal cloud that developed from the ejected atoms. This interaction produces surface oscillations that lead to nucleation of vortices [45]. Afterwards, originating from the edge, the vortices are seen to penetrate the bulk of the BEC (1.4- to 3.0-s images).

After a considerable time, the vortices eventually pass through the central part of the condensate (3.5- to 5.0-s images). Unlike the results that were reported in Ref. [43],

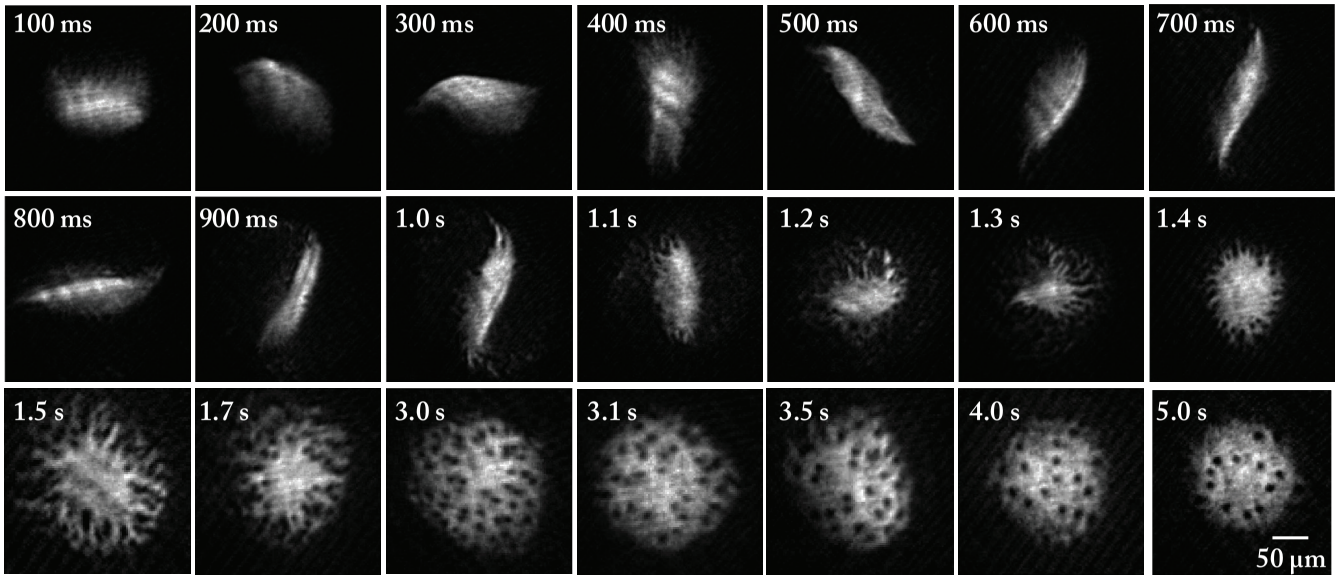

Figure 3.4 Evolution of highly oblate BEC during and after rotation of TOP trap. t = 0 is the beginning of the rotation. The total spin duration was 1 s at a frequency of 6.0 Hz. The elongation and distortion of the BEC is clearly seen as the spinning commenced. Some of the atoms get ejected out from the BEC forming low-density tails. Eventually, vortices are observed at the edge of the condensate as nucleation starts. Subsequently, the vortices penetrate the bulk of the BEC. A decrease in vortex number is noted as the vortices interact. A vortex lattice was not observed under any conditions that we examined.

we did not observe crystallization of the vortices into a vortex lattice. The vortices remained in a seemingly random disordered distribution across the condensate. It was also noted from the images that the number of vortices decreased with longer hold time.

On the other hand, there were no crystallizations that were observed in the numerical simulations that were reported in Refs. [34, 36, 45]. It was suggested in Ref. [34] that a longer waiting time will eventually lead to vortex lattice formation, as other dissipative mechanisms could affect lattice formation in 3D that are not present in 2D (such as vortex tilting, vortex recombination, etc.). It is also possible that due to the confinement of motion and interactions in only two dimensions, lattice formation would require longer time scales in our highly oblate trap [45].

As for the circulation direction of the vortices that remained in the condensate, there was no experimental method that was implemented to determine it. In the simulations of refs. [34, 43, 45], the vortices should have a single flow direction. Since the behavior of vortices that were observed in the experiment (from nucleation to migration to the BEC center) were consistent with those in the simulations, we speculate that the quantized vortices in the experiment also have a single circulation direction. Additionally, the only source for angular momentum in the system is the rotation of the trap; so it is expected that the net vortex flow would also have same the direction.

3.5 Summary

Rotation of Bose-Einstein condensates in a highly oblate trap was experimentally performed. This was accomplished by distorting the ellipticity of the magnetic radial trap and adding an oscillation frequency to give it a net rotation. The red-detuned laser sheet

that provided tight-confinement along the z-direction remained in place while the BEC was being rotated. Because of this, the condensate retained its highly oblate aspect ratio.

The effects of the different rotation parameters were investigated. It was observed that the number of generated vortices peaked around the vicinity of the critical rotation frequency (~5.65 Hz). A smaller ellipticity of the trap resulted into fewer vortices being generated and a longer rotation time was needed to create a sufficient number of vortices. It was noted though that longer spin times led to eventual heating of the condensate, which affected the lifetime of the vortices in the BEC. Due to the higher thermal non-condensate fraction, vortex damping was more pronounced and the number of vortices in the BEC decreased with longer rotation times.

The time evolution of the BEC during and after trap rotation were also observed through a set of images that were taken at different points along the rotation process. The dynamical instabilities that the BEC underwent were clearly observed. The onset of vortex nucleation at the edge of the condensate were visible in the images. It was also seen that these vortices eventually migrate towards the central region of the BEC. No vortex lattice was observed as was seen in other experiments [26, 28]. This lack of a vortex lattice may be attributed to the different kind of vortex dynamics that occurs in our highly oblate trap due to interactions being constrained in just two dimensions. Nevertheless, from this experiment, the creation of highly disordered distributions of singly quantized vortices of the same circulation sign in a BEC was shown to be possible. Because of this aspect, this method may prove useful in experimentally generating 2D quantum turbulence, wherein it can be characterized and analyzed in terms of intervortex separations and distances, as suggested in Ref. [46].

Additionally, due to the aspect ratio of our trap, the observation of vortex interactions and dynamics is potentially easier in nominally 2D than in 3D condensates. Since the vortex filaments remained straight along the z-axis, there was no ambiguity in identifying and distinguishing the vortices. Lastly, the final disordered arrangement of the vortices and the ease at which these can be observed give the system and the spinning process the possibility of being a test bed in studying quantum vortex dynamics, interactions, and turbulence.

CHAPTER 4

VORTEX FORMATION FROM AMPLITUDE MODULATION OF A BLUE-DETUNED OPTICAL POTENTIAL

This chapter discusses an experiment wherein the optical power of a focused blue-detuned laser beam that was incident in a highly oblate Bose-Einstein condensate (BEC) was modulated. Quantized vortices were immediately observed due to the amplitude modulation of the optical potential. The effects of time length of modulation, location in the BEC of the optical potential, and beam geometry is presented. A mechanism of vortex formation is also proposed.

4.1 Motivation

As described in Chapter 2 and in previous experiments [16], it has been shown that harmonic modulation of the radial trapping frequency of both a harmonic trap and a toroidal trap[1] led to the generation of quantized vortices in a BEC. Modulating the trap frequency of the harmonic trap generated vortices that appeared to originate from the edge of the condensate. On the other hand, vortices seemed to emerge from the toroidal center of the BEC, where a fixed blue-detuned potential wall is located, in the toroidal

[1] The toroidal trap geometry was experimentally achieved by adding a vertically propagating blue-detuned optical potential at the center of the harmonic trap.

trap geometry. What was interesting about these initial experiments was that symmetric harmonic modulations of the radial trapping frequency (which led to symmetric fluid flow in the BEC) were not expected to nucleate vortices by itself [19, 25, 29, 30, 53-59]. The physical mechanism on how vortices are generated in these experiments are certainly not yet clear; additional experiments and numerical simulations are necessary in order to provide a plausible explanation for the vortex formation process. Such experiments may also help in our understanding of the role of trap noise, rates of decoherence, and the roles of the thermal atomic background.

In order to further understand the mechanism in this symmetric modulation procedure, we studied a harmonic trap with a weak potential dimple at its center, and extended these experiments by evaluating what happened to the condensate when the strength of the relatively weak inner potential barrier is modulated instead of the outer potential wall. With this approach, it was intended to isolate the source where nucleation of vortices actually occur i.e. whether vortices were generated in the vicinity of the modulated surface of the condensate or around the fixed outer trap wall.

Furthermore, from the radial magnetic trap modulation experiments, it is apparent that highly disordered distributions of vortices in a BEC can be generated using radially symmetric modulation of the confining potential. If the weak potential modulation experiment that we are proposing in this chapter generates vortices, it is likely that a highly disordered distribution will also be generated. And since the modulation is symmetric, with no net angular momentum, the vortices that will be produced would have circulations in both signs. Hence, this technique may prove useful in experimental studies of 2D quantum turbulence.

This chapter is organized as follows: the next section gives a description of the experiment setup. Sections 4.3 and 4.4 discuss the different conditions that were tested out in this study and the results that were obtained. A hypothesis regarding the mechanism of vortex formation in this experimental process is proposed in Section 4.5. The final section provides a brief summary of this chapter.

4.2 Description of experiment setup

All of the experiments utilized highly oblate ^{87}Rb Bose-Einstein condensates, as obtained from the experiment procedure that was described in Chapter 2. To provide a weak potential barrier or dimple in this highly oblate harmonic trap, a vertically propagating (z-direction) blue-detuned optical potential was added. This blue-detuned laser beam (λ = 660 nm) is focused onto the BEC and has a $1/e^2$ radius of ~9.7 μm. A diagram of the optical system that was used to focus the blue-detuned beam onto the BEC is shown in Figure 4.1. The red-detuned flat laser sheet (λ = 1090 nm), which provided tight confinement along the z-direction, was also still present.

To facilitate modulation of the blue-detuned beam, a function generator (DS345, Stanford Research Systems) was attached to the current controller of the 660-nm diode laser. When triggered, the function generator provided a sinusoidal bias voltage to the current controller. The bias voltage V_{BIAS} from the function generator has two controllable parameters: sinusoidal wave frequency ν, and peak-to-peak voltage amplitude V_{PP}. For all of the different sets of parameters that were investigated, beam modulation always started at zero power (i.e. there is a $-\pi/2$ phase shift in the sine wave function provided by

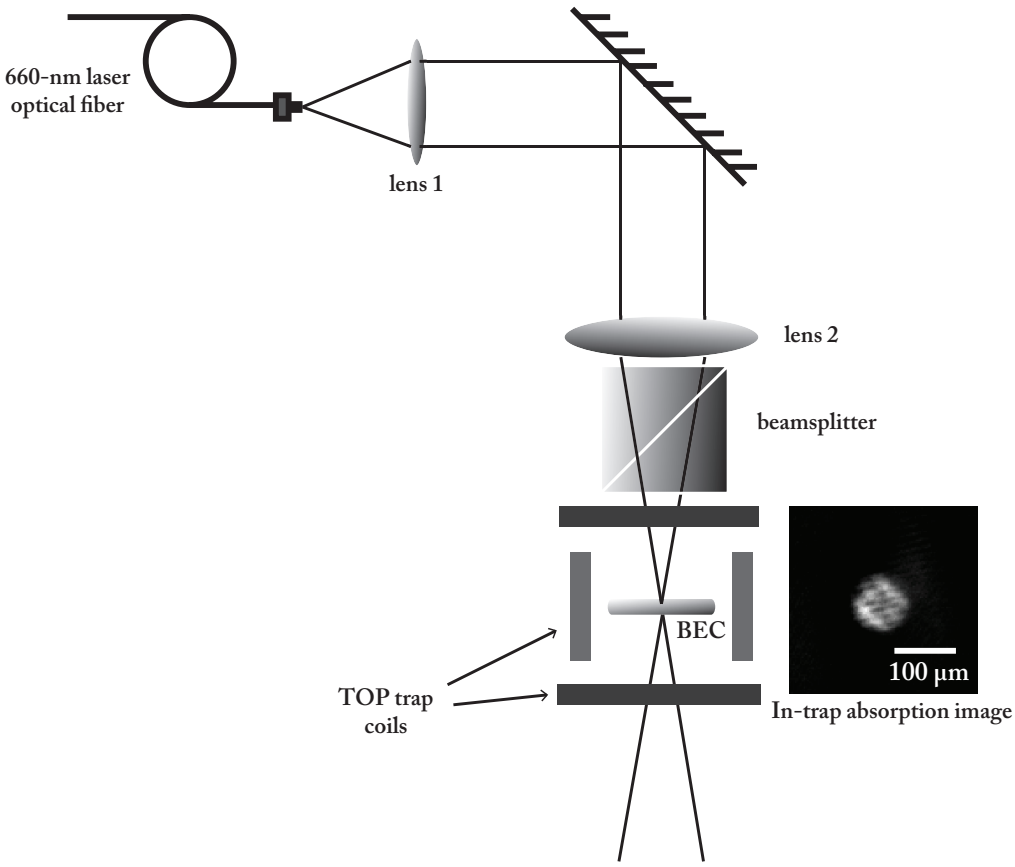

Figure 4.1 Schematic diagram of the optical system that was used to focus a 660-nm blue-detuned laser beam onto the BEC. Lens 2 has a focal length of 100 mm. Lens 1 is variable and acts as a collimator for the output beam from the optical fiber. Essentially, the focal length of Lens 1 determines the size of the focused beam on the BEC. The beam, propagating along the vertical axis, creates a repulsive barrier which penetrates the condensate, depending on the optical power. An image of an in-trap BEC with a blue-detuned beam at the center is shown. The power of the beam in this image is ~0.25μ_0, which is just enough to make a "dimple" on the surface of the BEC. (Note: not drawn to scale).

the function generator). A DC offset of $0.5V_{PP}$ is added to the bias voltage signal to ensure that negative voltage is not being provided to the current controller. Hence, the current controller received the following bias voltage:

$$V_{BIAS}(t) = V_{PP}\left[\frac{1}{2} + \sin\left(\nu t - \frac{\pi}{2}\right)\right]. \tag{4.1}$$

The resulting optical power of the blue-detuned laser beam has a linear relationship with the bias voltage that was provided by the function generator. While modulating the blue-detuned beam, the rf magnetic field jumps to a higher frequency[2] (~7.0 MHz) to prevent loss of atoms in the condensate.

4.3 Modulation of blue-detuned potential

The first set of parameters that was investigated were ν = 16.0 Hz and V_{PP} = 1.0 V. This gives a peak optical power of ~$0.25\mu_0$, where μ_0 is BEC chemical potential. The blue-detuned potential was located at the center of the harmonic trap. An in-trap absorption image of the BEC along the vertical imaging axis with the blue-detuned potential at peak power is shown in Figure 4.1.

Directly after rf-induced evaporation, the modulation of the beam was initiated. Three periods of oscillation of the beam power was performed i.e. a total time duration of 187.5 ms. Afterwards, with the blue-detuned potential at zero power[3], the BEC was held

---

[2] The frequency of rf-induced evaporation typically ends at ~ 4.8 MHz.

[3] The duration of modulation was always chosen such that the blue-detuned beam starts and ends with zero power, to prevent excitations in the condensate that are not brought about by the modulation. It is also possible to create vortices if the blue-detuned beam is instantly turned on to maximum power or instantly removed.

in the trap at variable increasing lengths of time. Subsequent to this, the condensate was allowed to expand and an absorption image of the expanded BEC was taken along the vertical imaging axis.

Figure 4.2 shows a set of absorption images of the expanded BEC at the end of each hold time. This set is meant to show snapshots of the time evolution of the BEC after modulating the blue-detuned optical potential at its center. Each image is taken in increments of 10-ms hold time, directly after beam modulation up to 140 ms. Due to the destructive nature of the imaging process in the system, it should be noted that each image consisted of a different BEC, albeit subjected to the same blue-detuned potential and modulation parameters. Despite this limitation, this set of images is representative of the behavior of the condensate as it evolved after beam modulation.

From these images, it could be seen that directly after beam modulation (i.e. no hold time), the expanded BEC did not seem to expand to any larger size at all. In fact, from post-processing of the image, the expanded BEC after beam modulation has a measured Thomas-Fermi (TF) radius of ~57.5 μm, which is approximately equal to the TF radius of the condensate when held inside the harmonic trap. Nevertheless, as the BEC was held further in the trap, the expanded BEC was observed to oscillate in size (see Figure 4.3, hollow circles). TF radius measurements of the condensate from in-trap absorption images also revealed oscillatory behavior in condensate size (see Figure 4.3, filled squares). Additionally, based on curve fitting procedures, the oscillation frequency of the BEC radius is approximately 14.8 Hz, which is approximately twice the radial trap frequency. It is also the modulation frequency of the optical potential, chosen such that near resonant excitations of atoms in the trap might occur locally. Looking further into

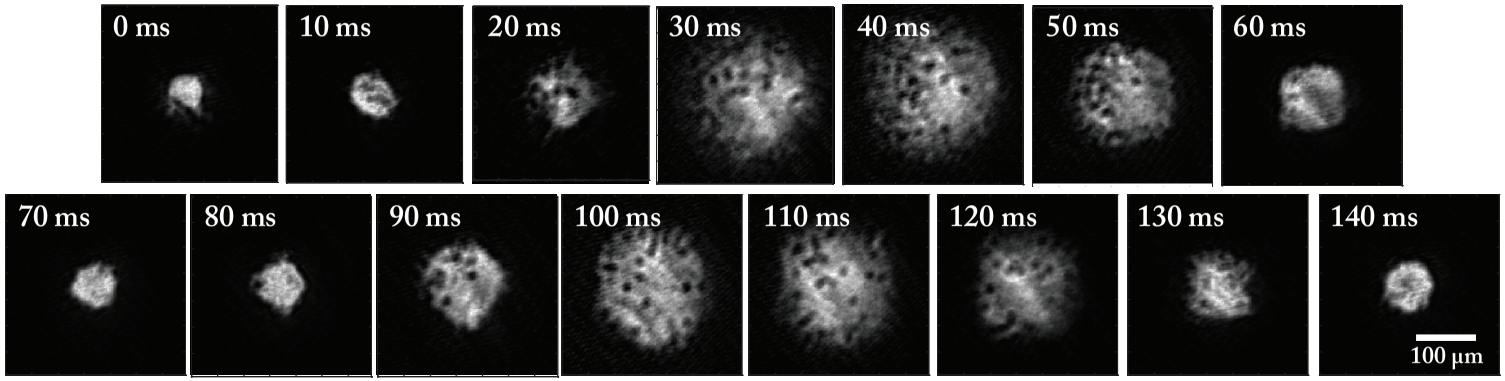

Figure 4.2 Evolution of the highly oblate condensate after three cycles of modulation of the blue-detuned beam's optical power. These are absorption images of expanded BECs taken at 10-ms intervals of hold time after beam modulation. The oscillation frequency was 16 Hz, and the maximum optical power of the blue-detuned potential was ~0.25μ_0. The BEC size oscillates after beam modulation with an approximate period of 70 ms. The size oscillation is accompanied by generation and apparent annihilation of vortices inside the BEC.

the evolution of the BEC, we took images of the expanded condensate up to 2.07 s with 70-ms intervals. Measurements of the TF radius of the condensate from these images showed damping of the size oscillation amplitude (Figure 4.4). At long wait times, the oscillations should be negligible and looking at the plot, the radius damped out to ~100 μm, which is the typical radius of an expanded BEC in this trap.

More interestingly, singly quantized vortices were also observed inside the condensate. From the images in Figure 4.2, it could be noted that there are significant changes in the number of vortices inside the BEC as it evolved after modulation of the blue-detuned potential. There were instances along this time evolution that the BEC had no resolvable vortices inside, and then vortices emerged and seemed to increase in number. Afterwards, the amount of vortices seemed to decrease. This cycle in vortex number continued afterwards. From images taken after longer hold times (up to 2.0 s), vortices were still observed inside the BEC.

Based on these observations, it would seem apparent that there was continuous vortex nucleation and vortex annihilation or damping within the BEC. The mechanism for nucleation is not clear since there was an symmetric modulation of the condensate based on its size oscillations. The apparent short lifetime of vortices in this particular system cannot be attributed alone to thermal damping [13, 28, 54, 60-65]. This high rate at which vortices disappeared from the condensate suggests the possibility that vortex-antivortex annihilation was occurring within the BEC. This, of course, suggests that vortices of opposite circulations were both generated with this process, as should be the case for any symmetric process that does not add net angular momentum to the system. With our imaging methods, it was not possible to verify this conjecture that vortices of opposite

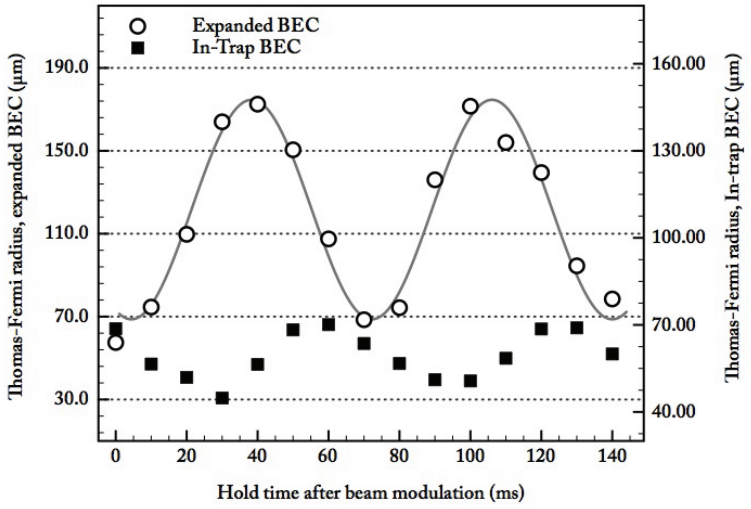

Figure 4.3 Time evolution of the Thomas-Fermi radius of the expanded (hollow circles) and in-trap (filled squares) Bose-Einstein condensate after a 16.0-Hz modulation of the blue-detuned potential for 3 cycles. The BEC exhibited size oscillations with a frequency of ~14.8 Hz (from a sinusoidal fit [solid line]). The size oscillations of the BEC in the trap and after expansion manifested opposite behavior due to the ballistic nature of the expansion process. These oscillations were accompanied by nucleation and removal of quantized vortices in the condensate, as seen from the images in Figure 4.2.

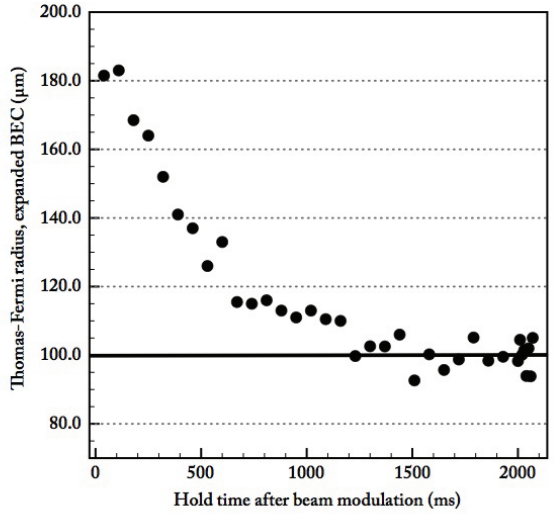

Figure 4.4 The envelope of the oscillation of the TF radius of the expanded BEC after modulation of the optical power of the blue-detuned beam. As discussed in this chapter, the BEC oscillates in size after beam modulation. The data points that are depicted here correspond to the largest TF radius at each oscillation cycle. The size oscillation eventually damps out to a typical TF radius (i.e. no beam modulation) of an expanded BEC from this trap (~ 100 μm, indicated by the solid horizontal line).

winding were created by beam modulation.

A higher modulation amplitude V_{PP} was also investigated; a 2.5-V oscillation was chosen. This gave a maximum optical power of ~0.50μ_0 to the blue-detuned beam. An in-trap image of the BEC with the blue-detuned potential at the center is shown in Figure 4.5, with the dip in the condensate density at the center of the BEC being more pronounced due to the higher optical power. Using the same values for the other oscillation parameters, the time evolution of the condensate after beam modulation was observed, and is shown in Figure 4.5. Similar to the behavior that was seen in the case of lower peak power, oscillation in BEC size was also detected. What was notable is that the amount of vortices that was generated was also higher. This could be attributed to the faster effective rate of change in the optical power of the blue-detuned beam.

4.4 Effect of the location and geometry of the blue-detuned potential

In the two cases that have been discussed in the previous section, the source location of the nucleation process for the vortices was not apparent from the images, with the vortices spread out within the condensate. Whether nucleation originates from the outer edge of the condensate or from the potential dimple at the center could not be determined. In order to address this issue, the location of the beam was moved off-center into different locations inside the BEC. The in-trap absorption images of the condensate with the off-center blue-detuned potential are shown in figures 4.6a-c. Modulation of the beam occurred at these positions (indicated by the white arrows).

For these experiments, the oscillation parameters that were used are: ν = 16.0 Hz and V_{PP} = 1.0 V. To further isolate vortex generation from the effects of multiple oscilla-

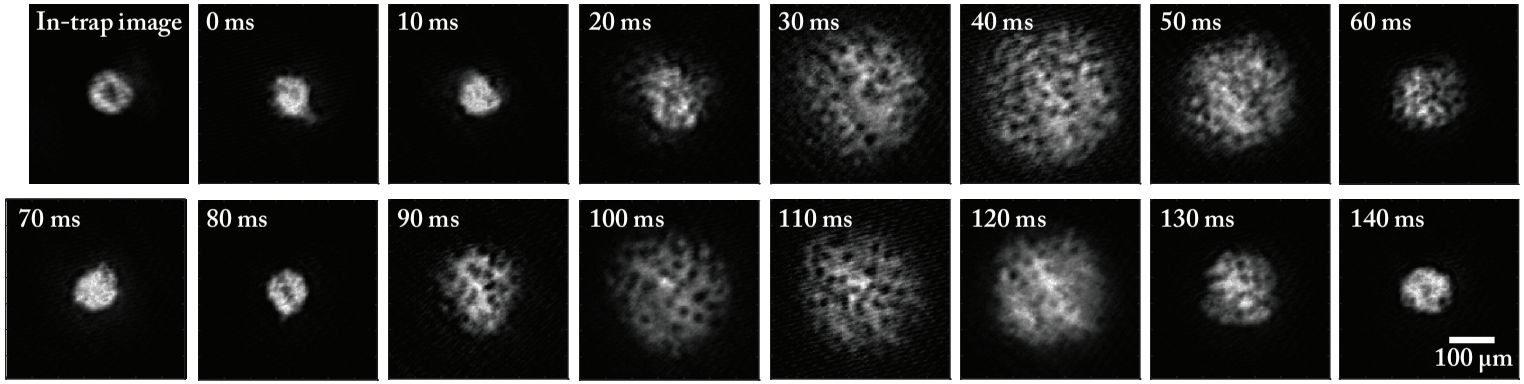

Figure 4.5 Evolution of the highly oblate condensate after three cycles of beam modulation at a higher optical power. The first image is an in-trap BEC image with a deeper density dip at its center due to the higher strength of the blue-detuned potential. These are absorption images of expanded BECs taken at 10-ms intervals of hold time after beam modulation. The oscillation frequency was 16 Hz, and the maximum optical power of the blue-detuned potential was ~0.50μ_0 mW. A higher number of vortices was generated as compared to when the blue-detuned beam has a lower optical power. The in-trap image is the same scale as the expanded BEC images.

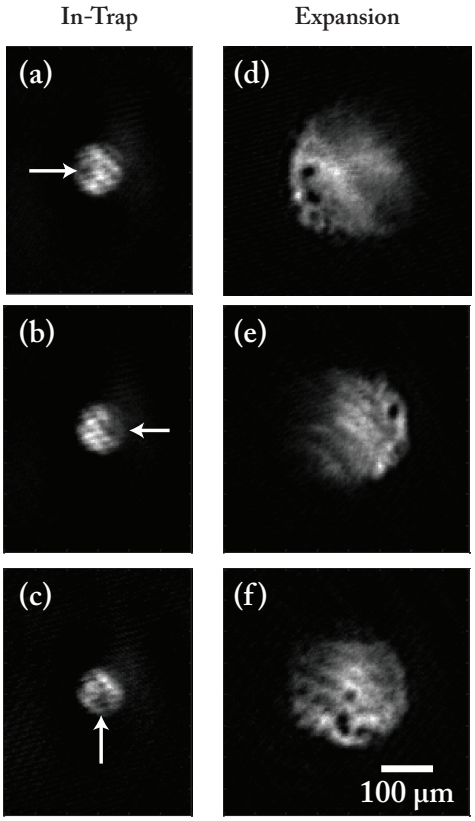

Figure 4.6 Effect of the position of the modulated blue-detuned beam in the condensate to vortex generation. Shown here are (a)-(c) in-trap and their corresponding (d)-(f) expansion absorption images of the BEC. The blue-detuned beam was taken off-center to different locations in the condensate (indicated by a white arrow), where a single oscillation was then performed. It was observed that the vortices present in the expanded BEC were concentrated on the vicinity of the beam position.

tions in the BEC size, the beam was modulated for a total of one cycle only (62.5 ms). The BEC was then held in the trap for 40 ms;[4] afterwards, it was allowed to expand and an absorption image was taken. These images (figures 4.6d-f) show that the vortices in the BEC were located in the vicinity where the beam was located in the condensate. This localization in vortex position suggests that vortices were nucleated at the location of the modulated barrier.

This localization effect of the position of the blue-detuned potential on vortex formation prompted us with the idea that controlled localization of vortex formation is possible.[5] It is conceivable to have a collection of points in the condensate where modulated blue-detuned potentials can be positioned to act as nucleation centers.

An upper limit for this collection of nucleation centers is a set of points that are very close to each other; the simplest way that this could be experimentally realized is by having an elongated blue-detuned "line" potential. We demonstrated this possibility by changing the geometry of the blue-detuned beam; instead of a focused Gaussian-shaped spot, the weak blue-detuned potential was changed to a focused blue-detuned laser sheet. This was accomplished by adding a cylindrical lens directly before the final focusing lens in the blue-detuned laser beam optical path. For simplicity, the beam was positioned along one of the transverse axis of the condensate.

---

[4] From the time evolution images of the BEC in the previous section, it was evident that at ν = 16.0 Hz, the largest size that the condensate was able to reach and had the most number of vortices was after a 40-ms hold time. For this reason, the images were taken after this length of wait time.

[5] A new method of controlled positioning of vortices in a BEC is discussed in Chapter 7 of this dissertation.

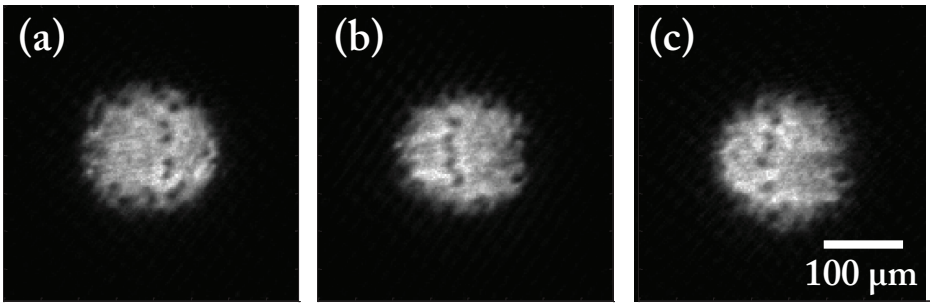

Figure 4.7 Absorption images of expanded BECs after modulation of a blue-detuned "line" potential. An elongated blue-detuned beam was initially incident along one of the transverse axis of the BEC. The beam was then modulated at a frequency of 16 Hz for one period. At the beginning and end of the modulation, the beam was at zero power. After 40 ms of wait time, the BEC were allowed to expand and absorption images were taken. Vortices were observed along the axis of modulation in a linear configuration. Note that vortices also appear along the outer edge of the BEC.

Because the laser beam that was incident to the condensate is more spread out than a focused Gaussian-shaped beam, the V_{PP} that was used was 3.5 V (corresponding to an optical power of 15 mW) in order to maintain the same amount of beam penetration into the BEC density. A modulation frequency of 16.0 Hz was used for a total of one oscillation (62.5 ms). A 40-ms hold time was again used after the modulation of the potential. Figures 4.7a-c show absorption images of the BEC after expansion. As expected, these images clearly show that vortices were localized along the length of the blue-detuned potential within the condensate. As was proposed in the preceding paragraphs, a line of nucleation centers was created as evident from the line of vortices that were observed at the center of the BEC.

4.5 A plausible explanation for vortex nucleation

Several things were clear from the above experiments. Nucleation of vortices occurs at the vicinity where the condensate density was modulated by the blue-detuned potential. The number of generated vortices increased when the modulation was higher. Also, the general configuration of the vortices follow the geometry of the modulation amplitude in the condensate density. An apparent continuous process of nucleation and removal of vortices were also observed after modulating the power of the laser beam. Also, vortex nucleation was achieved in these experiments without forced rotation of the condensate or any other method that involved a direct and apparent transfer of angular momentum into the BEC.

Unlike in previous vortex formation experiments that involved forced rotation, either by laser-beam induced spinning [25-27, 48] or rotating magnetic traps [30, 31, 66], there was no unidirectional fluid flow in our system. One possible mechanism of vortex formation from beam modulation might be associated with the relative motion of the condensate fraction with the thermal non-condensate part and brought about by mutual friction and counterflow between these two components. This mechanism has been studied in fluid interface studies (both in classical fluids and superfluids) and is called the Kelvin-Helmholtz instability [67, 68]. This instability happens along the interface of two fluids that have relative velocity and gives rise to the nucleation of vortices in the interface of the two fluids. The instability has been shown in the interface of two phases of superfluid ^{3}He [67], and has recently been attributed as the vortex formation mechanism for an oscillating trapped BEC as it interacts with the thermal cloud [69, 70].

We speculate that near-resonant beam modulator drives the BEC atoms into excited states, causing a local depletion of the superfluid component. As superfluid in the nearby regions fills in the depleted region, there may be thermal counterflow due the locally energized atoms moving away from the modulation site. This thermal counterflow may produce vortices, as is the case in superfluid helium [71-73]. However, detailed numerical simulations should be performed to confirm this vortex nucleation hypothesis.

4.6 Summary

An experiment was described in this chapter that involved a sinusoidal modulation of the strength of a focused, blue-detuned weak optical potential within a Bose-Einstein condensate. Oscillations in the size of the BEC were observed after modulation of the optical potential; these oscillations were accompanied by a continuous process of formation and annihilation of quantized vortices in the BEC. The number of generated vortices were directly dependent on the strength of modulation. Vortex formation is localized in the immediate vicinity of the optical potential. Due to this dependence of vortex nucleation on the position of the blue-detuned beam, the geometry of the potential determined the general clustering configuration of the vortices being generated. Although it was not confirmed through experiment, vortices of opposite circulations were believed to be generated in this method due to the short lifetimes of the vortices and the absence of transfer of net angular momentum in the BEC excitation process.

The complete mechanism of vortex nucleation in this experiment is not yet fully understood; a Kelvin-Helmholtz instability in the interface of the condensate and the thermal background is regarded as the most plausible process. Further experiments and

numerical simulations that will take into account the interaction of the BEC with the non-condensate part would be beneficial in understanding the vortex nucleation mechanism in this system.

Lastly, the oscillations of the BEC size that were observed in these experiments may prove to be a limitation in using this technique as a vortex-generation method for experimental studies of quantum turbulence. Due to these size oscillations, vortices will not be resolved by the imaging system when the BEC is at its smallest size, and vortex dynamics, intervortex separations, and vortex interactions cannot be observed. For future refinements of this method, it is suggested that a possible minimum optical power for the blue-detuned beam is investigated such that vortex generation is still possible with minimal or no oscillation in BEC size. It is also possible that the sequence or timing of the amplitude oscillations of the optical beam may be modified to prevent the observed size oscillations in the BEC.

CHAPTER 5

QUANTIZED VORTICES WITH HIGH WINDING NUMBERS

This chapter describes a newly developed experimental technique to generate quantized flow of multiple vorticity in highly oblate ^{87}Rb Bose-Einstein condensates. This novel method involves translating an axially propagating, blue-detuned, Gaussian-shaped laser beam along a spiral trajectory on the transverse plane of the condensate, starting from the edge of the BEC and moving towards its center. The resulting amount of vorticity can be varied with a certain degree of control and depends on the rate of translation.

5.1 Motivation

One aspect of vortex studies in BECs is the fast rotating regime where a so-called "giant vortex", or a multiply quantized vortex, gets created. Several numerical and theoretical studies have explored the formation of this giant vortex from fast rotation [74-78], and involved the initial creation of a vortex lattice and the use of magnetic traps that are tighter than harmonic to induce the formation of the multiply quantized vortex. Several experimental methods were also devised to achieve a multiply quantized vortex in a BEC. This is due to the difficulty in achieving this type of superflow in a superfluid helium [79]. A giant vortex was achieved experimentally from a lattice by selective removal of atoms in

the BEC [31]. Another method involved the topological imprinting of phase in the BEC through adiabatic inversion of a magnetic bias field along the condensate trap axis [80-84]. In this method, the highest winding number achieved was four. Another method is the transfer of orbital angular momentum of Laguerre-Gaussian beams into the condensate atoms [85-88]. This method can potentially achieve high winding numbers, but only doubly quantized vortices have been experimentally realized so far. To achieve higher amounts of vorticity, a vortex pump was theoretically proposed, and this involved cyclic operation of the topological phase imprinting method [89, 90]. This method has yet to be implemented in experiments. Another aspect of these multiply quantized vortices is their stability. It has been known that they are highly unstable in harmonically trapped nonrotating condensates [82, 91-93], such that they immediately decay into singly quantized vortices. To maintain their circulation, a pinning potential is necessary and is usually implemented using a blue-detuned optical beam [81, 84, 86, 87].

Multiply quantized vortices are of interest in superfluid research because they can open up possibilities in studying phase slippage [76, 94] and also the dynamics of the stability and decay of these giant superflows. The capability to control and generate the amount of vorticity that can be achieved from these multiply quantized vortices could lead to new experimental and systematic studies on fast rotation of superfluids.

Additionally, the instability of these multiply quantized vortices in the absence of pinning potentials can be used to launch singly quantized vortices of the same circulation sign inside a BEC. With this capability, experiments that require a specific number of vortices in a particular circulation direction may become realizable. Also, experiments involving interactions of a specific number of oppositely charged, singly quantized vortices

may be performed if multiply quantized vortices of opposite circulation can be produced within a BEC. From such controlled experiments, our understanding of basic vortex interactions may improve and can be built upon to explore their relevance to 2D quantum turbulence.

Based on the above reasons, it is then quite essential to develop an experimental method that is able to generate superfluid flows of high circulation numbers, smoothly transition to stabilizing this multiply quantized flow, and eventually, induce instability that will cause the multiply quantized circulation to break into singly quantized vortices. In this chapter, we present such a technique that we have developed.

This chapter is arranged as follows: the next section gives the details of the newly developed method to generate multiply quantized vortices. Sections 5.3 discusses the different conditions and parameters that were tested out in this study and the results that were obtained. The final section provides a brief summary of this chapter.

5.2 Experimental description of technique

We started with a highly oblate ^{87}Rb Bose-Einstein condensate utilizing the formation procedure discussed in Chapter 2. Upon the end of the rf-induced evaporation sequence, the center of the magnetic trapping potential was translated by R_0 = 75 μm along the horizontal (x) direction using a magnetic push coil. This BEC movement was done relatively slowly within 500 ms.

In addition to the vertically confining, red-detuned (λ = 1090 nm) laser beam, we included a repulsive optical potential that penetrates the condensate and propagates along the vertical (z) axis. This blue-detuned (λ = 660 nm) laser beam was focused onto the

BEC; it had a $1/e^2$ radius of ~18 μm and a maximum total power of ~ μ_0, where μ_0 is the BEC chemical potential. The optical setup for this blue-detuned beam is similar to the one used in the previous chapter (see Figure 5.1). Upon shifting the center of the harmonic magnetic trap, the power of the blue-detuned beam was linearly increased from zero to its maximum total power in 500 ms. The position shift of the harmonic trap placed the initial location of the blue-detuned beam just outside the BEC boundary.

The condensate was then translated along a spiral trajectory by shifting the center of the magnetic trapping potential using two magnetic push coils, oriented along the *x*- and *y*-axes. The blue-detuned optical beam remained stationary while moving the BEC. In the rest frame of the condensate, the blue-detuned beam would be tracing out a spiral path within the BEC. This spiral trajectory $S(t)$ is described by the parametric equations:

$$r(t) = R_0\sqrt{1-\frac{t}{t_S}} \tag{5.1}$$

$$\theta(t) = 2\pi N\left(\frac{t}{t_S}\right)^2, \tag{5.2}$$

where $r(t)$ is defined as the radial distance of the center of the blue-detuned beam from the center of the BEC, and $\theta(t)$ is the beam's angular displacement with respect to the axis defined by its initial position and the center of the BEC. The variable N is the number of revolutions within the spiral and t_S is the total time of the trajectory. This trajectory was chosen since it approximates the behavior of the speed of sound in the condensate i.e. low near the edges and a maximum at the center. The effective path of the blue-detuned

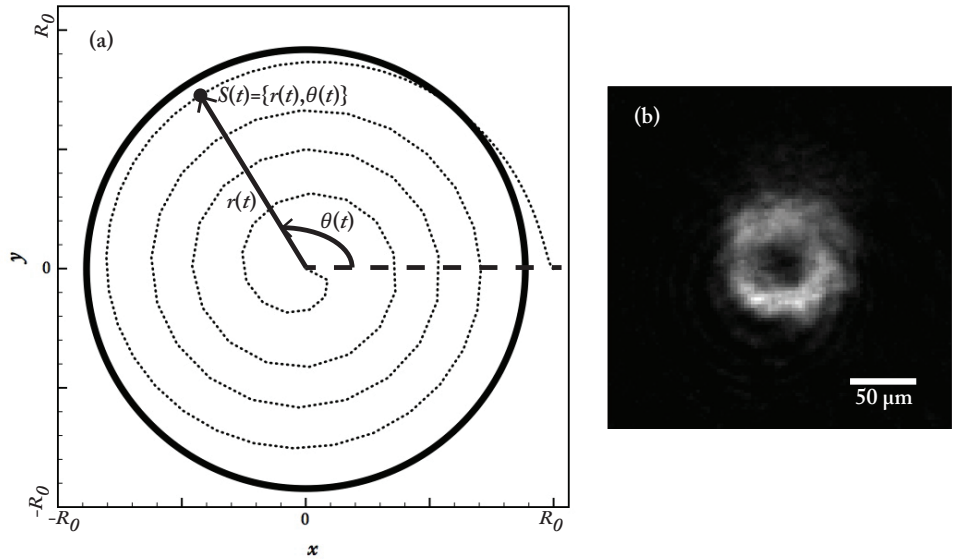

Figure 5.1 (a) A diagram of the spiral trajectory $S(t)$ that the blue-detuned optical beam effectively traces out in the BEC as the condensate is moved around by the magnetic push coils for $N = 4$ turns. It is determined by two time-dependent parameters $r(t)$ and $\theta(t)$, as defined in Eqs. (5.1) and (5.2). The beam starts from the edge of the BEC and ends at its center. The solid circle approximates the edge of the BEC. (b) An in-trap absorption image of the BEC (taken along the vertical imaging axis). The density dip at the center of the condensate is due to the presence of the blue-detuned optical potential. This marks the end position of the beam in the spiral trajectory.

beam with respect to the condensate is shown in Figure 5.1a. As depicted here, the blue-detuned beam eventually ends up in the center of the condensate. Figure 5.1b shows an in-trap absorption image of the BEC with the blue-detuned beam in its center, seen as a circular gap in the BEC.

After a subsequent variable hold time t_H, the power of the blue-detuned beam was decreased linearly to zero. The magnetic trapping potential was turned off and the BEC was allowed to expand in the red-detuned optical trapping potential for 10 ms. The red-detuned beam was then removed and the BEC was allowed to expand further for 35 ms. A vertical absorption image of the condensate was then taken.

5.3 Experimental results

5.3.1 Creation of a giant vortex

Shown in Figure 5.2a is a transverse absorption image of the BEC that was taken immediately after the blue-detuned optical beam is removed and ballistic expansion has occurred. For this particular BEC image, the parameters used in the experiment were $N = 4$, $t_S = 5.0$ s, and $t_H = 3.5$ s. As can be observed, a large circular gap was present in the center of the condensate. It should be noted that the blue-detuned beam was no longer present in the system when the image was captured; hence, the existence of a hole in the BEC could not be attributed to the presence of a blue-detuned potential. Instead, the circular gap in the BEC is interpreted to indicate vorticity, which suggests that fluid flow was occurring in the condensate.

The size of the hole in the BEC should be worthy of note. When compared to the size of a vortex core having a single quantum of circulation (e.g., as those typically observed in vortex lattices), the size of the gap in the condensate density was much larger. Therefore, we could conjecture from this observation that the winding number of the vortex produced by the beam-spiral method is more than unity. Note however that the presence of the large hole after expansion does not automatically mean that a multi-quantum vortex was created in the BEC. In other words, we cannot (and do not try to) distinguish between a single vortex with a winding number of q, and q singly quantized vortices that are close enough together before expansion that their cores overlap during expansion. However, with a pinning beam on, the two situations are basically the same since the vorticity is pinned to the optical potential.

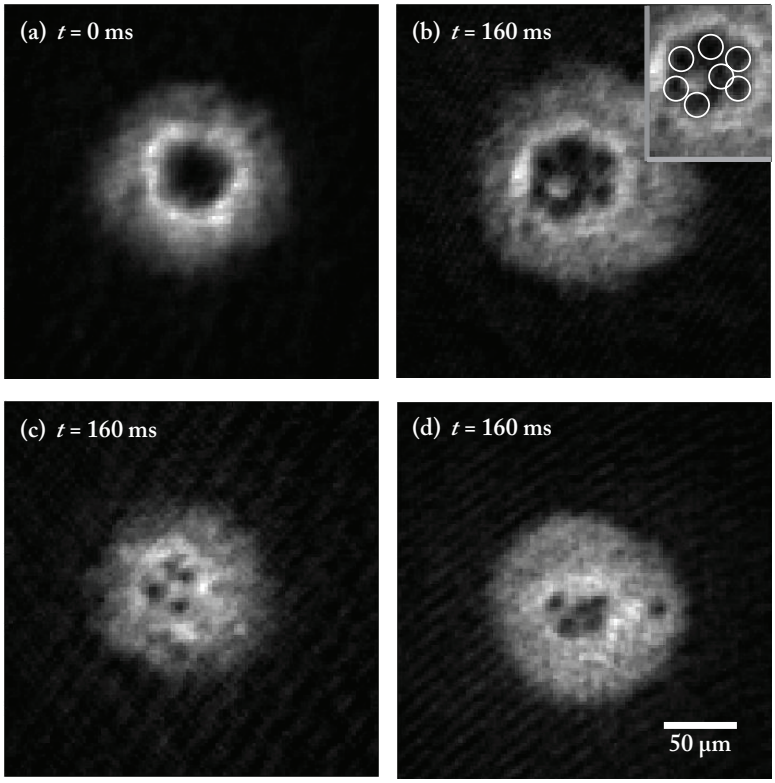

Figure 5.2 Absorption images of the expanded BEC (along the vertical imaging axis) subsequent to the beam spiral process (a) with no extra wait time and (b) with 160 ms of hold time between turning off the blue-detuned beam and expansion. Directly after moving the blue-detuned potential along the spiral trajectory and after expansion, a large circular gap in the condensate density was located at the BEC center, and is interpreted as the core of a giant or multiply quantized vortex. When expansion is initiated 160 ms after the end of the spiral process, the giant vortex dissociated to singly quantized vortices due to the absence of a pinning potential (blue-detuned beam). The parameters for this the spiral trajectory are N = 4, t_S = 5.0 s, and t_H = 3.5 s. *Inset*: Magnified image of the singly quantized vortices. The white circles indicate an individual vortex core. From this image, seven singly quantized vortices can be resolved. (c)-(d) Expanded BECs that show different numbers of singly quantized vortices, depending on the translation speed of the blue-detuned beam.

In order to verify this and to quantify the circulation number of the vortex that was produced with this technique, we held the condensate in the combined magneto-optic trap for an extra 160 ms after turning off the blue-detuned optical beam but right before expansion and imaging. In doing so, we allowed the vortex state in the BEC to evolve without the blue-detuned pinning potential. It has been shown that a multiply quantized vortex state is unstable [91, 92, 95-97], and in the absence of a pinning potential, will tend to dissociate into singly quantized vortices. This is because the energy of a vortex with more than one unit of circulation is greater than the energy of a collection of singly quantized vortices with the same total circulation; hence, multiply quantized vortices will not exist in equilibrium in a harmonic trap [17]. Unlike in numerical simulations wherein the circulation number of a vortex can be easily quantified by looking at the phase map of the condensate, direct observation and measurement of the phase of a BEC in the experiment using our imaging methods is not possible. Instead, the dissociation of the multiply quantized vortex into individual vortices of unit circulation would be used to quantify the vorticity that was generated by the beam-spiral technique.

With the added hold time prior to expansion, we were able to observe individual singly quantized vortices in the condensate through absorption imaging, as seen in Figure 5.2b. These vortices were localized at the center of the BEC, where the multiply quantized vortex was located. This suggests that the individual vortices were from the dissociation of the giant vortex because the pinning potential was no longer present. From the image, a total of seven singly quantized vortices could be resolved; hence, the circulation number of the multiply quantized pinned vortex that was generated through this particular sequence was approximately seven.

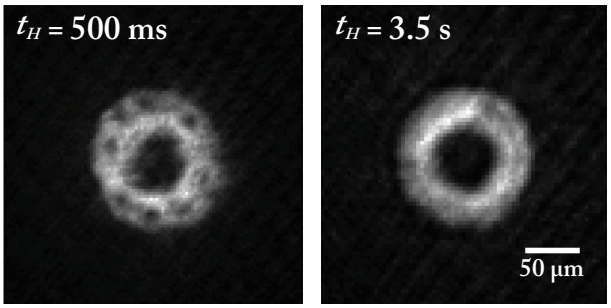

Figure 5.3 Existence of unpinned vortices after the beam-spiral technique. These are absorption images of expanded BECs with different hold times t_H between the end of the spiral process and removal of the pinning potential. At t_H = 500 ms, there are several visible vortex cores that are located off-center in the BEC. These vortices are considered to be unpinned. At longer hold times (t_H = 3.5 s), these unpinned vortices eventually leave the condensate, and the pinned multiply quantized vortex is left at the BEC center.

5.3.2 Existence of unpinned vortices

The results that were discussed in the previous subsections were taken with a significantly long hold time (parameter t_H = 3.5 s) between the end of the spiral trajectory and the start of the blue-detuned beam's power ramp-off. Figure 5.3 shows a comparison of condensates with two different t_H values. It could be noted that at t_H = 500 ms, there were numerous singly quantized vortices in the BEC, in addition to the multiply quantized vortex at the center. We treated these singly quantized vortices as unpinned since they were not held in place by the blue-detuned potential. On the other hand, at t_H = 3.5 s, the only vortex in the BEC was the pinned vortex with multiple circulation quanta.

It was evident from these two images that some vortices that were produced during the beam-spiral process did not get pinned to the blue-detuned beam. The additional hold time in the trap was essential to allow vortices that were not pinned to leave the condensate and to achieve a BEC that has only a multiply quantized vortex. Due to the

finite temperature of the system, the non-condensed thermal atomic cloud was a source of dissipation [63] and helped in the process of eliminating the unpinned vortices. The interaction of the unpinned vortices with this thermal cloud caused damping of these excitations in the BEC. With an appropriate amount of hold time, the fluid circulation that remained in the condensate was that of the giant vortex alone, which was pinned to the blue-detuned potential.

5.3.3 Controlling the amount of vorticity

The effect of the rate at which the blue-detuned optical potential was translated along the spiral trajectory was also investigated, in terms of the resulting amount of circulation in the generated vortex. We varied the translation speed by fixing the parameter N to a constant value ($N = 4$) and modifying the time parameter t_S. Figure 5.4 shows a plot of the behavior of the circulation number of the generated vortex when t_S was changed. The statistical data from the experiment are depicted in filled circles, while results from numerical 2D-GPE simulations are shown in hollow squares with a dashed line. At zero temperature, the experiment is simulated using a 2D-GPE, as described in section 1.3. The potential due to the blue-detuned beam was modeled in the simulations as $U(x,y,t) = U_0 \exp\left\{-2\left(\left[x - x_0(t)\right]^2 + \left[y - y_0(t)\right]^2\right)\Big/ w_0^2\right\}$, where $U_0 \sim 0.5\mu_0$ and $w_0 \sim 18$ μm. The time-dependent spatial coordinate variables are defined by the spiral trajectory described in eqs. (5.1) and (5.2).

Each experimental data point in this plot is an arithmetic mean of 10 runs, with the error bars showing the standard deviation of the observations. The circulation number

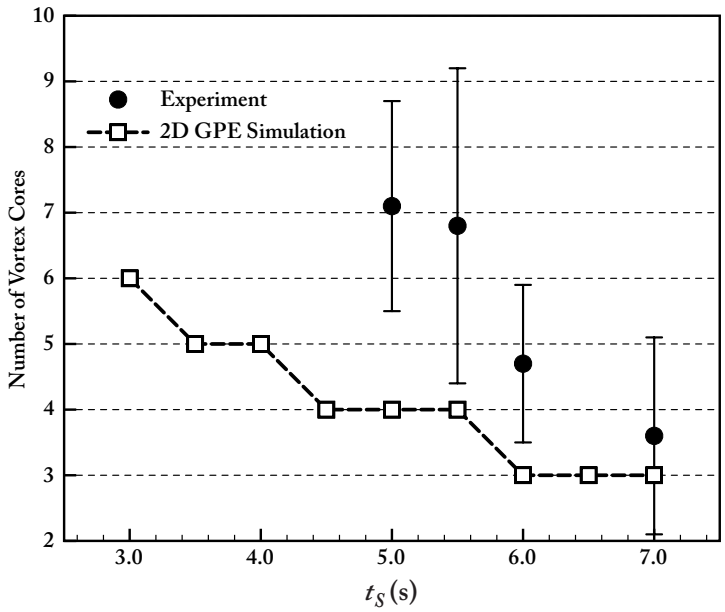

Figure 5.4 Plot of the circulation number of the resulting multiply quantized vortex as the trajectory time t_S was varied. A decrease in the winding number was observed in both the experiment (filled circles) and 2D-GPE numerical simulations (hollow squares) with longer trajectory durations. Each experimental data point represents an arithmetic mean from 10 trials, and the error bars are standard deviations of the observations.

of each multiply quantized vortex was quantified by using the method that was discussed in section 5.3.1. Four values of t_S were used in the experiment: 5.0 s, 5.5 s, 6.0 s, and 6.5 s. From the plot, it could be seen that with a slower rate of moving the blue-detuned beam (i.e. a longer trajectory time t_S), the amount of circulation in the generated vortex decreased.

The numerical GPE simulations of the beam-spiral process have yielded an identical behavior. Despite having the same trend of decreasing vorticity with slower translation rates, the circulation numbers obtained with the simulations are generally lower than those from experiment. We attribute this slight discrepancy between the two data sets to

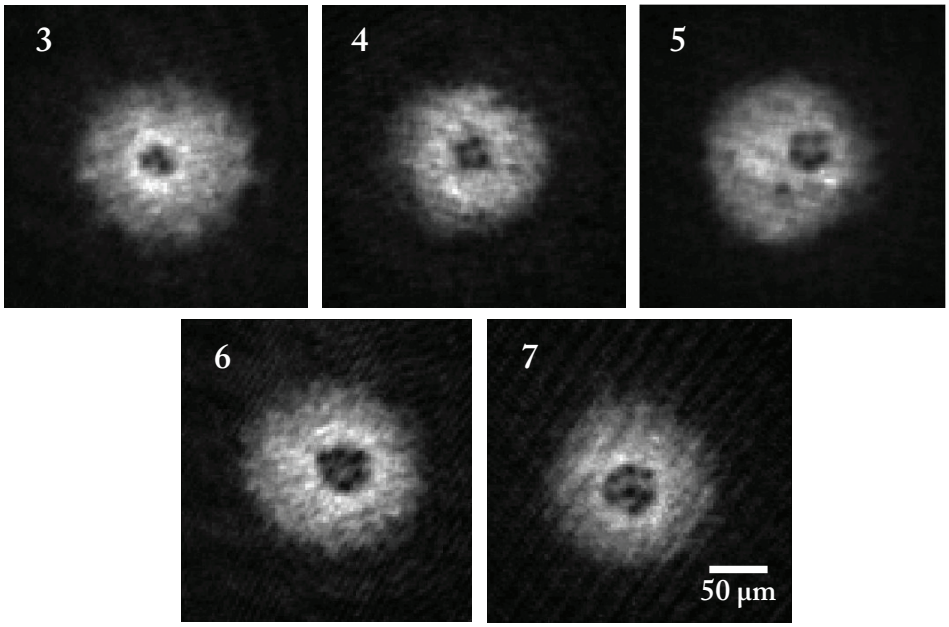

Figure 5.5 Regular vortex array patterns from the dissociation of the multiply quantized vortex. On a few instances, after linearly ramping off the blue-detuned optical potential and waiting a few milliseconds to allow the multiply quantized vortex to dissociate into singly quantized vortices, regular patterns of these vortex clusters were observed. The interaction of the vortices that brought about these structures are not yet fully understood, and may be related on how the pinning potential was ramped off. The stability of these structures can be of interest. The indicated number in each absorption image of the BEC is the number of singly quantized vortices in the vortex array pattern.

possible incongruities between parameters in the numerical simulations and the actual conditions in the experiment. It is plausible that during the experiment, the spiral trajectory that was traced out by the blue-detuned optical beam was not entirely coincident within the boundaries of the BEC. If the trajectory is slightly off from the confines of the condensate, there are instances that it can perturb the boundary of the BEC more than once, which can contribute further in the generation of vortices. Additionally, mismatch of the mapped-out trajectory to the actual location in the BEC may result to higher-

than-desired speeds for the blue-detuned potential; this will eventually lead to an increase in the vortex number.

Nevertheless, both simulations and experiment support the notion that the rate at which the blue-detuned potential is moved along the spiral path has a direct effect on the circulation number of the pinned vortex that can be generated with this technique. Specifically, both approaches show that faster motion along the spiral trajectory leads to a higher winding number. This characteristic of the technique can be utilized to acquire some degree of control when generating a desired vorticity for any quantized flow in a BEC.

5.3.4 Other notable results: Regular vortex patterns after dissociation

In a few of the experimental trials in which the circulation number was quantified, regular array configurations of singly quantized vortices were observed following dissociation. Representative images of these regular arrays for different circulation numbers are shown in Figure 5.5. These are reminiscent of vortex array patterns that were initially observed in superfluid helium [79].

The interaction of the vortices that brought about these structures are not yet fully understood, and may be related on how the pinning potential was ramped off. Recently, a numerical study has analyzed the dependence of these vortex arrays on the parameters of a Gaussian pinning potential [98]. The conditions for stability of these structures can also be of interest. Further experiments and numerical simulations are highly suggested to understand the dynamics that are involved here.

5.4 Summary

In this experiment, we have proposed and demonstrated a new technique that can generate a multiply quantized vortex state in a highly oblate Bose-Einstein condensate. This novel method involved moving a focused blue-detuned optical potential from the outside of the BEC and towards its center along a spiral path. The circulation number of the generated vortex depended on the speed of the optical potential, with faster motion leading to a higher amount of vorticity. The generated multiply quantized vortex was always located at the center of the BEC, which was the end position of the blue-detuned optical potential, and suggested that vortex pinning transpired in the system. In a few instances, regular array configurations of singly quantized vortices were observed after the pinning potential was linearly ramped off; this experimental result supports the idea that this vortex-generation technique may prove beneficial in studies involving vortex-vortex interactions and vortex-impurity interactions. Furthermore, due to the tendency of the multiply quantized vortex to disintegrate into singly quantized vortices on the absence of a pinning potential, this method may prove useful in preparing BECs that contain a specific number of singly quantized vortices having the same circulation sign.

CHAPTER 6

VORTEX TWEEZERS: HIGHLY CONTROLLED GENERATION AND MANIPULATION OF QUANTIZED FLOW

In this chapter, a new experimental method of creating singly quantized vortices of opposite circulation in a Bose-Einstein condensate is presented. The technique involves the use of two independently moving blue-detuned optical potentials. Controlled manipulation of the vortices in terms of their position within the BEC is also demonstrated.

6.1 Motivation

From the experiments in the previous chapters, it is evident that the topic of vortex dynamics in highly oblate condensates is quite of interest and is open to a lot of research possibilities. Vortices in this system can be easily detected by conventional imaging methods for dilute gas BECs. Because vortex filament bending is inhibited, the possibility of two detected vortex cores being the two ends of a twisted filament is essentially zero. This makes the analysis of vortex-vortex interactions in these highly oblate condensates from images more tractable and relatively less complex. Furthermore, because of the strong asymmetry between the radial and axial trapping directions, vortex line motion is confined to two dimensions, and excitations having a three-dimensional nature are suppressed [10, 12, 16]. Therefore, the vortex dynamics and interactions are said to be two-

dimensional and different from those in a three-dimensional system, which is typical of most previous BEC experiments.

The best approach in understanding these 2D vortex dynamics is to acquire the ability to engineer any kind of vortex state that we desire to study. In doing so, a more controlled, thorough, and systematic way of studying vortex dynamics and interactions can be implemented. As an example, if we desire to start every experiment trial with the same initial vortex configuration in order to build up and quantify the desired statistics of their interaction, the capability of repeatably creating this initial vortex configuration in a BEC will be extremely useful. The capacity to engineer arbitrary vortex patterns or configuration will also be beneficial since different experimental conditions can be tested out.

The most basic strategy to achieve vortex engineering capabilities is to have a procedure that can create and manipulate singly quantized vortices in a condensate, as a singly quantized vortex is the most basic unit of fluid flow in a BEC. If we can deterministically generate a singly quantized vortex and then manipulate it into any location within the BEC, and perform this in succession, creating and re-creating an arbitrary vortex configuration can be experimentally realizable. Such a method to perform vortex engineering will be truly useful and important.

The method in the previous chapter has shown that pinning of vortices can be achieved with a blue-detuned potential, and that the amount of vorticity can be deterministically controlled to a certain degree. This can be considered one technique in engineering a vortex state in a BEC. In this chapter, we present another vortex generation method, that reliably creates singly quantized vortices, with the added capability of vortex manipulation.

This chapter is organized as follows: the next section gives a description of the experiment setup. Sections 6.3 discusses pertinent details of the experimental results and capabilities of the newly developed vortex creation and manipulation method. The final section provides a brief summary of this chapter.

6.2 Experimental description of technique

As in previous chapters, a highly oblate ^{87}Rb Bose-Einstein condensate in the combined optical and magnetic trap was utilized in this second deterministic vortex-generation method. In this technique, we used two focused blue-detuned optical beams to nucleate and afterwards, manipulate the position of the vortices inside the BEC. Unlike the method that was described in the previous chapter, movement of the optical beams with respect to the condensate were not accomplished by translating the BEC; instead, this was achieved by utilizing scanning mirrors that directly deflect the optical beams. With this configuration, there would be better control and independence of movement for the two beams. In addition, the condensate was not needed anymore to be translated by magnetic bias fields and remained stationary within the trap.

Figure 6.1 shows a schematic diagram of the optical system that was used to control the movement of the blue-detuned beams in the condensate. The 660-nm laser beam was fed into this optical system from an optical fiber output coupler. The laser beam then passed through a polarizing beamsplitter; the two outgoing orthogonally polarized beams served as the focused blue-detuned optical potentials for the experiment. Each output beam then bounced off a set of two mirrors, which controlled the deflection and motion of the beams within the BEC that were necessary for this technique. The pair of mirrors

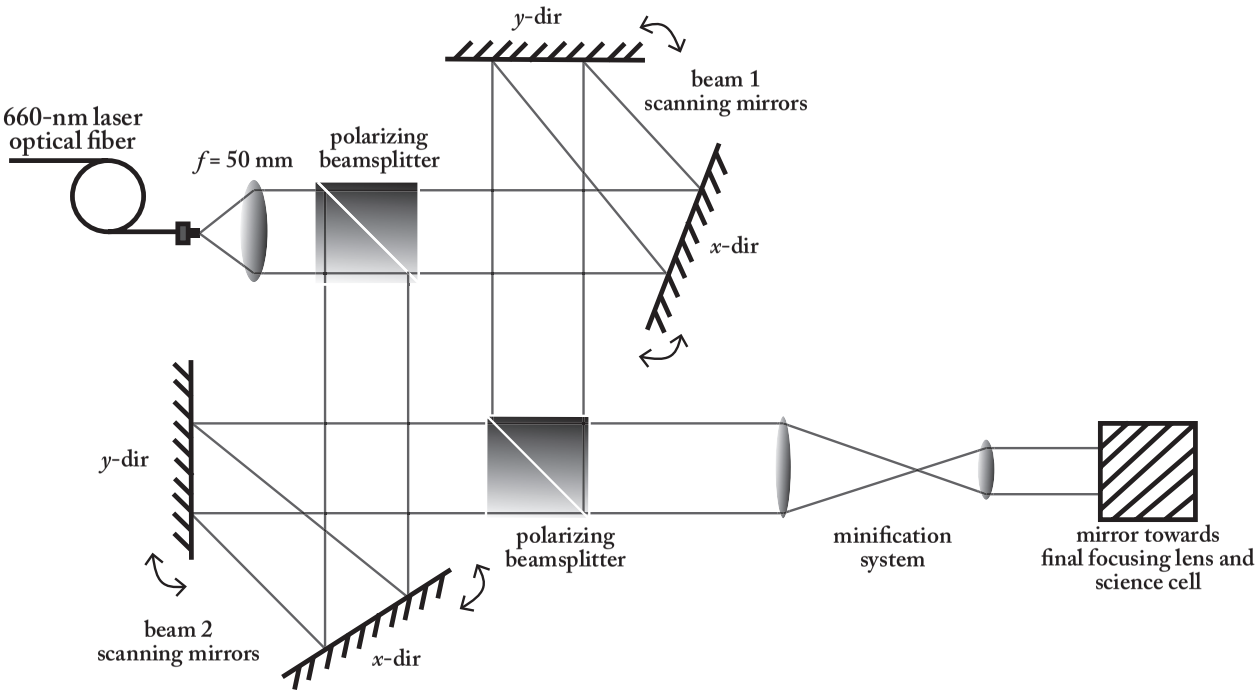

Figure 6.1 Schematic diagram of the optical system that was used to translate two blue-detuned optical potentials across the BEC. This setup replaces the optical fiber and lens 1 components in the setup found in Figure 4.1. The 660-nm laser beam is split into two by the first polarizing beamsplitter. Each branch goes to a set of two mirrors, which controls the movement of the beam in the BEC. This was done by attaching PZTs to one adjustment screw in each mirror mount. One mirror controls movement in one transverse direction. The two beans are then recombined in the second polarizing beamsplitter. A variable minification system is used to control the size of the focused beams in the BEC.

in each set were configured such that one mirror controls the movement of the focused laser beam along one transverse axis. This was accomplished by attaching a piezoelectric transducer (PZT) to one of the adjustment screws in each mirror mount. With these four scanning mirrors, the two blue-detuned beams could be moved anywhere in the transverse plane of the BEC independently from each other.

Upon emerging from their respective set of scanning mirrors, the blue-detuned beams were recombined by another polarizing beamsplitter. Minimal interference between the two beams was expected due to their orthogonal polarizations. This recombined beam then passed through a beam minimizer, which controlled the size of the focused beams in the BEC. For the experiments described in this work, a 6× and a 3× minification systems were used. Finally, the recombined beams passed through the 100-mm lens that focused them into the condensate.

In order to accommodate the use (i.e. ramp-on, ramp-off, initial positioning, etc.) of these two blue-detuned beams, and because the vortex-creation method required that these beams are initially located inside the condensate, the BEC formation procedure that was described in Chapter 2 was given a slight modification. Specifically, a two-stage rf-induced evaporation process was utilized. This refinement in the condensation method was implemented in order to prevent the unintended formation of vortices when linearly ramping on the two optical beams. Directly after loading the non-condensed thermal cloud into the flat red-detuned beam, the first stage of rf-induced evaporation commenced and occurred for 6 s. At the end of this stage, a condensate with a relatively significant thermal cloud fraction was produced. An in-trap phase-contrast image along the horizontal imaging axis of the condensate after this intermediate evaporation stage is

shown in Figure 6.2a. After a 500-ms wait time, the two blue-detuned beams were then linearly ramped on to full power (~ $0.8\mu_0$ each) in a span of 2.5 s, where μ_0 is the BEC chemical potential. The two beams were initially coincident and were located ~10 μm away from the center of the BEC. Afterwards, the second rf-induced evaporation stage began, in which the usual condensate fraction was achieved. The duration of this second evaporation was 2.5 s. An in-trap horizontal phase contrast image of the condensate after this second evaporation stage is shown in Figure 6.2b. As can be seen, the thermal non-condensate component was reduced after this second stage. An in-trap vertical absorption image of the BEC is shown in Figure 6.2c with the two blue-detuned beams at their initial position and coincident with each other.

To generate vortices, the two beams were slowly translated across the condensate and were separated at the same time. The trajectories *P1* and *P2* (having lengths l_1 and l_2, respectively) in Figure 6.2e illustrate the paths that the beams traced out in the BEC. The two paths make an angle α_P between them, and are symmetric with each other with respect to the axis of propagation of the red-detuned optical sheet. These beams were swept across the BEC at a variable time t_P. The final positions of the blue-detuned beams in the BEC are shown in Figure 6.2d.

At this point, a singly quantized vortex was expected to have been nucleated and pinned in each of the blue-detuned beams, based on 2D-GPE simulations of the methods, similar to the simulation method described in the previous chapter. If desired, the two beams could be moved to any location in the condensate and are independent of each other, using the scanning-mirror system. If pinning is indeed successful, the vortices should move together with the beams. To facilitate the observation of these vortices and

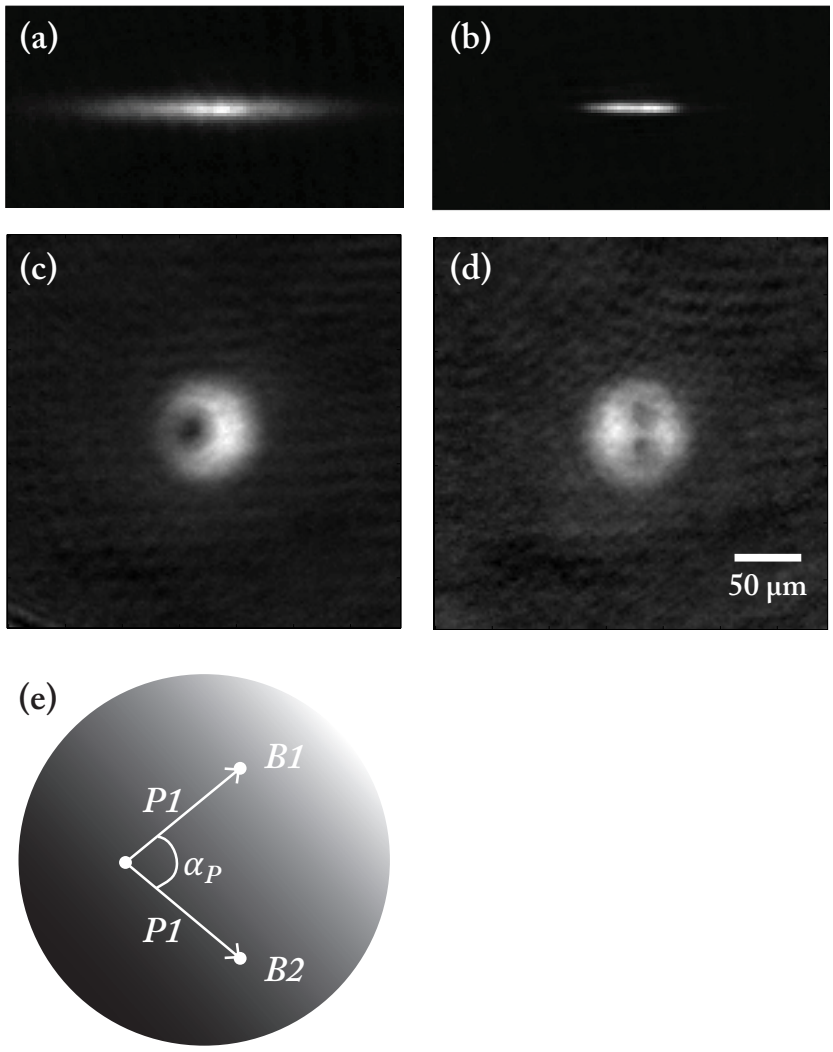

Figure 6.2 In-trap phase contrast images of the BEC (along the horizontal imaging axis) right (a) after the first stage of rf-induced evaporation and (b) after the second stage. There is still a significant amount of thermal component after the first stage of evaporation to ensure minimal creation of unwanted vortices when the blue-detuned beams are ramped on. In-trap absorption images of the BEC (along the vertical imaging axis) with the two blue-detuned optical beams at their (c) initial and (d) final positions. The beams are seen as density dips in the condensate. (e) A schematic diagram of the beam trajectories inside the BEC. The two beams share a common initial position, and eventually separate during the vortex creation process.

their locations in the condensate with respect to the end positions of the blue-detuned potentials, the powers of the two beams were linearly decreased to zero in 250 ms. The rate of the beam power ramp-off was determined experimentally such that it was fast enough to ensure that the vortices would not drift away as the beam power is decreased and that they remained at their positions prior to beam ramp-off, but slow enough such that no further excitations in the condensate occur. Expansion and imaging of the BEC directly followed after turning off the blue-detuned beams.

6.3 Experimental results

6.3.1 Repeatable creation of singly quantized vortices

A 6× beam minimizer was initially used in the beam-scanning system that was described in the previous section. With this configuration, both of the focused blue-detuned beams in the condensate have a $1/e^2$ radius of ~19 μm. The paths *P1* and *P2* that were traced out by the blue-detuned potentials each have lengths of ~28 μm. The angle α_P between them was ~67°. The beams were swiped for t_P = 700 ms. Figures 6.2a and 6.2b show a typical BEC with the blue-detuned beams for these experimental parameters.

After swiping both beams across the condensate, the BEC was held in the trap for variable time durations, with the two beams fixed at their final positions and their powers held constant. Thereupon, the blue-detuned beams were linearly ramped off in 200 ms. The BEC was then allowed to expand, and absorption images were taken along the vertical imaging axis.

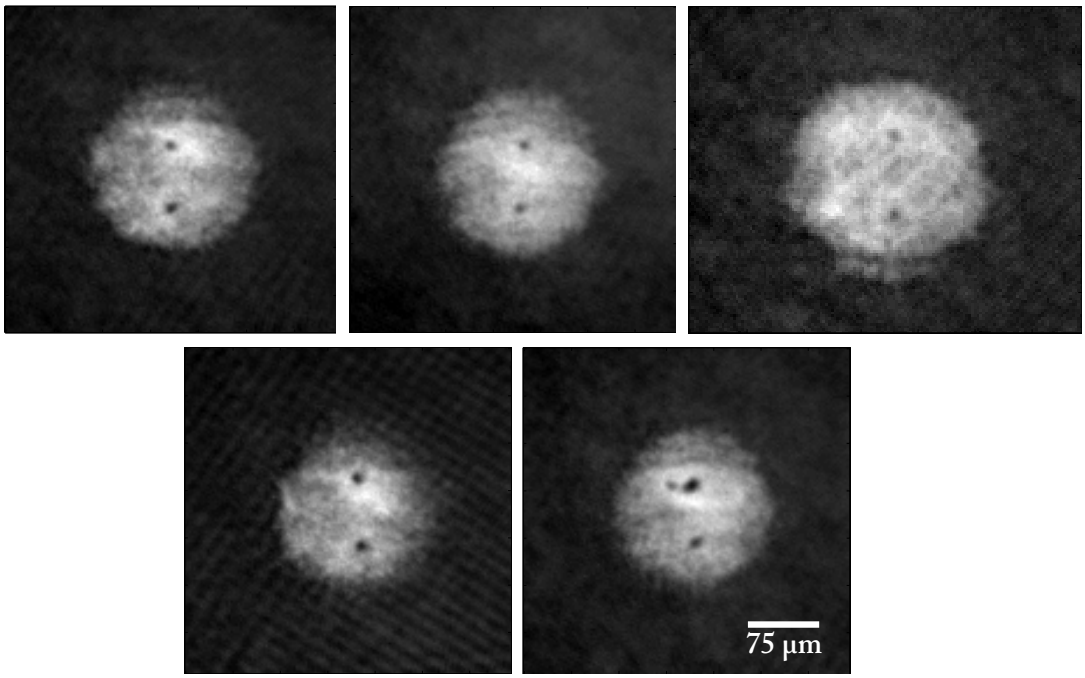

Figure 6.3 Absorption images of expanded BECs (taken along the vertical imaging axis) after the two blue-detuned beams were slowly swiped across the condensate. As can be seen, two vortices were created by the method. From a set of 30 BECs, the method generated exactly two vortices approximately 87% of the time. Each vortex was located at the end position of one of the beams. In the other 13% of the cases, either only one vortex was located in the BEC, or an extra unpinned vortex was observed, in addition to the two vortices.

An absorption image of an expanded condensate that underwent this vortex-generation method with the above parameters is shown in Figure 6.3. It could be noted that this BEC contained exactly two vortices. From the image, the size of the vortex cores were those of singly quantized vortices. Additionally, the locations of the two vortices in the condensate were approximately in the end positions of the two blue-detuned beams, with one vortex corresponding to one beam.

To ensure that the vortices were generated by this beam-swiping method alone and not through ramping off the blue-detuned potentials, the beams were initially placed

in the endpoints of paths *P1* and *P2*, and the revised BEC formation protocol, beam ramp-on, and beam ramp-off as outlined in section 6.2 was performed, sans the beam swiping. No vortices were generated from this procedure. The same check was done for beam ramp-on by placing the beams in the starting points of *P1* and *P2* and not moving them. Again, no vortices were observed from this procedure.

To demonstrate replicability, the beam-swiping method was repeated consecutively 30 times, and obtaining exactly one singly quantized vortex at the end position of each blue-detuned potential was achieved 87% of the time. On the other 13% of the cases, the BEC either had only one vortex (located on one of the pinning sites), or an extra unpinned vortex was observed in the BEC, in addition to the two vortices that are located on the end positions of the two beams. It should also be noted that in the cases wherein exactly two vortices were generated, the expanded images of the BECs from the replications look almost exactly the same (see Figure 6.3), despite being different BECs due to the destructive nature of the observation and imaging process. Furthermore, the method was repeated for the same experimental parameters and conditions in succeeding trials for several days, with favorable results. From these observations, it could be safely stated that the method is robust and approximately has 90% repeatability.

In a previous study that also involved swiping of a blue-detuned potential, and also produced two vortices [10, 16], the mechanism was vortex shedding when the moving obstacle exceeded a particular critical speed. The speed of the two beams in our experiment is 40 μm/s, which is below the critical speed (~ 170 μm/s) to nucleate vortex dipoles by vortex shedding.[6] Hence, no vortices should be expected from this translation

[6] This value of the critical speed was taken from Refs [10, 16] since the system in this study and in those references are exactly the same.

speed. Despite this, two vortices were reliably generated with the method. How does this method generate vortices?

When the two beams start moving, they induce fluid flow in the condensate. If we follow the diagram in Figure 6.2e, the fluid at the vicinity of the two beams gets pushed towards the right. We should note that the trajectories of the two beams bifurcate but because the two beams are not point-like but have finite sizes, it would still appear as if they are connected. Effectively, at the early part of their trajectories, an elongated blue-detuned obstacle is moving towards the right. Fluid near the center of the obstacle is constantly pushed and eventually flows around the obstacle. Hence, the initial flow will be counterclockwise at the top of *B1* and clockwise at the bottom of *B2*. As the obstacle eventually separate into two distinct beams, a small channel opens up between them, and the fluid gets to flow continuously around each beam, and a closed circular flow can be established. Thus, the circulation around *B1* is counterclockwise, and clockwise for *B2*. From this analysis, it can be inferred that the two vortices that were repeatably reproduced in the above results have opposite circulation.

Another way of looking at this method is that as the two blue-detuned beams separate and a tiny channel opens up between them, the small gap gets filled up with atoms, albeit a lower density. Essentially, this forms a localized soliton in between the two blue-detuned beams. Because it is dynamically unstable, the soliton should decay into a vortex-antivortex pair [99, 100]. The close proximity of either vortex to one of the blue-detuned beams causes the vortex to be drawn towards the center of the repulsive potential, and allows the vortex to be captured and pinned [101]. The experimental observation of this pinning and vortex manipulation is discussed in the next subsection.

6.3.2 Pinning and dynamic manipulation of vortices

The results from the previous section have hinted that pinning of vortices has been achieved with this vortex-generation method. This could be inferred from the observation that the generated vortices were always located in the final position of the blue-detuned optical potentials. To further scrutinize if pinning is achieved in the process, and as stated earlier, the BEC was held in the trap for variable time durations after beam-swiping and while keeping the strength of the blue-detuned potentials constant. These hold times ranged from 500 ms to 2.5 s.[7] Despite changing the duration of the hold times, the two vortices were located at exactly the same position as the final location of the blue-detuned beams, subsequent to expansion and imaging. This suggests that the blue-detuned beams can hold onto the vortices at variable time lengths, and that vortex pinning was indeed achieved with the method.

Because the capability to pin vortices was demonstrated, it was now possible to work towards accomplishing vortex manipulation (in terms of vortex position in the BEC) by utilizing the blue-detuned optical potentials. To demonstrate this capability, the following procedure was performed. After swiping the blue-detuned beams along paths *P1* and *P2*, they were held in the end positions of these paths for 500 ms. Afterwards, one of the beams were translated to another position, while keeping the other beam fixed. In our experiments, we translated one of the beams back to its initial position (starting point of either *P1* or *P2*) in 1 s. Following this, the beams were once more fixed in their

[7] The longest length of time that we could hold the BEC in the highly oblate trap while maintaining constant beam powers was limited by hardware constraints.

positions for another second, prior to ramping off the beams and expanding and imaging the BEC.

Figure 6.4a shows an in-trap image of the BEC with the two blue-detuned potentials after moving the upper beam (*B1*) back to its initial position and keeping the lower beam (*B2*) fixed. After taking an absorption image of the expanded condensate (Figure 6.4b), it could be observed that two singly quantized vortices were again present in the condensate as expected, but one of them was now located at a different position. One vortex core was still located at the position corresponding to that of *B2*, but the other vortex was now situated at the location where *B1* was moved.

From this observation, it can be inferred that after swiping the beams along *P1* and *P2*, two singly quantized vortices were generated, with one vortex pinned to each beam. By moving one of the beams relatively slowly, the corresponding pinned vortex was transported together with its pinning potential. As such, one of the vortices changed its location, while the other remained in place. A similar procedure was executed with *B1* being fixed and moving *B2* back to its initial position (Figure 6.4c). A similar result was obtained with one vortex staying on one site, while the other vortex (corresponding to *B2*) changed its location (Figure 6.4d). These results were clear indications that the position of a pinned singly quantized vortex inside a condensate could be controlled easily by slowly translating the position of its pinning potential. Because the blue-detuned pinning potentials in our system could be easily translated in any transverse location within the BEC by any combined deflections of the four scanning mirrors, the pinned vortices could be placed in any position in the condensate. Additionally, it could easily be conceptualized that this method could be scaled to consecutive movements of each beam, which

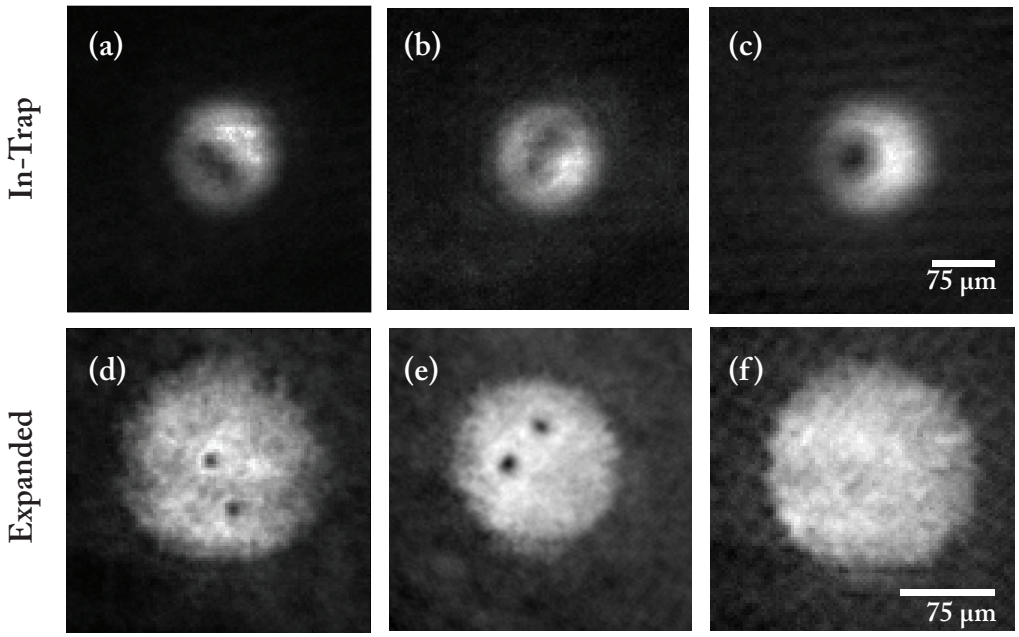

Figure 6.4 Demonstrating the vortex pinning and vortex manipulation capabilities of our newly developed method. After creating the two vortices using the method described in Section 6.2, the blue-detuned beams were moved to a different location: (a) the upper beam was moved to its initial position while the lower beam remained in place and (b) vice versa. Upon expansion, it was observed that the vortices moved with the beams, as shown in the (d)-(e) corresponding absorption images, suggesting that position of the singly quantized vortices can be manipulated using our method. (c) When the beams are made coincident once more, the vortices annihilate each other (since they have opposite circulation) and (f) the resulting condensate did not contain any vortices.

would result to arbitrary configurations of the two vortices inside the BEC.

With this in mind, the blue-detuned beams were moved one at a time in succession to demonstrate this capability. After generating and pinning the vortices (beams at endpoints of *P1* and *P2*) and waiting for 500 ms, *B1* was translated back to its initial position in 1 s, while *B2* was stationary. Directly after this, *B2* was then moved back to its initial position in 1 s, while *B1* remained stationary. At this point, the two beams were once more coincident (Figure 6.4e). After ramping off the beam and expanding and imaging the BEC, the resulting condensate contained no vortices (Figure 6.4f). Repeating this procedure yielded the same results.

From the discussion of the mechanism of this method in the preceding sections, it was mentioned that the two vortices that would be generated using this technique would always have opposite circulation, i.e. a vortex and an antivortex. Having this in mind and with the procedure mentioned in the preceding paragraph, moving the blue-detuned beams together into one location would result to having a pinned vortex move within close proximity to a pinned antivortex. This would result into a vortex-antivortex annihilation, which was evident by the lack of vortices in the expanded BEC. This simple experimental check verified two ideas: that indeed, a vortex and an antivortex would always be generated by this beam-swiping method, and that moving the blue-detuned beams in succession was possible and could move the vortices in any location within the BEC with any configuration.

6.3.3 Other experimental notes: Effect of beam width

In the previous subsections, each of the blue-detuned beams has a $1/e^2$ radius of ~19 μm. A smaller beam size was also tested out, in the presumption that it would provide a finer spatial resolution in the positioning of vortices. The 6× beam minimizer in the beam-scanning system was replaced by a 3× minimizer. Both of the resulting blue-detuned beams in the condensate from this modified optical system have a $1/e^2$ radius of ~10 μm.

The procedure was once more repeated with 30 consecutive trials. With the smaller beams, the repeatability of the method went down to 70%. It is possible that due to a smaller beam size, pinning the vortices to the blue-detuned potential was more difficult. It has been shown numerically that vortex pinning is highly dependent on beam width and beam intensity, and that there is a lower bound in these parameters that would allow for vortex pinning [101]. In this theoretical study, vortex precession due to the harmonic trap dominates the interaction between the vortex and the pinning potential for small beam widths.

6.4 Summary

In this chapter, a new experimental method to generate two singly quantized vortices of opposite circulation signs in a Bose-Einstein condensate by swiping blue-detuned laser beams across it was described and demonstrated. What sets this novel technique apart from other vortex-generation methods that also use beam swiping is the high level of control in the creation and positioning of the vortices. Additionally, the technique for creating vortices and manipulating them involved only a single experimental setup, and

no mechanical transition or apparatus change was needed to shift from vortex creation to vortex manipulation. This method utilized two blue-detuned optical potentials that were swiped across the condensate, which reliably resulted to generating two singly quantized vortices. These two vortices are each pinned to one blue-detuned beam, which gave this method the capability to easily manipulate the position of the vortices after their creation. Because of the immense flexibility and ease in moving the position of the two beams, the vortices can be practically placed in any location within the condensate. Additionally, both circulation directions are produced in this technique. This new method provides a straightforward but deterministic procedure of generating and controlling the position of vortices in a BEC with a relatively simple experimental setup. From this experiment, we have demonstrated an initial step towards engineering arbitrary vortex distributions in a BEC.

CHAPTER 7

CONCLUSIONS

This concluding chapter provides a short review of the important highlights from each experiment that was described in this dissertation.

7.1 BEC stirring in a highly oblate trap

The rotating trap experiments that were used to create vortex lattices in previous BEC experiments have been recreated, albeit in a highly oblate trap configuration. Trap rotation was performed while the BEC is confined in a red-detuned laser sheet. The evolution of the vortices in the condensate from their nucleation to their migration towards the BEC center were observed in a relatively good temporal resolution. No vortex lattice was formed in the highly oblate trap. Our results were able to complement several numerical simulations that involved rotation of BECs in a similar trap configuration. This technique of generating vortices may prove useful in experimental characterizations of quantum turbulence in terms of intervortex separations by preparing BECs with highly disordered vortex distributions.

7.2 Modulation by a blue-detuned potential

Vortices were generated in a BEC by a weak blue-detuned potential that is located within the condensate and whose optical strength was sinusoidally modulated. Due to the apparent lack of direct angular momentum transfer in this method, we assumed that the vortices are a mix of opposite circulations. Vortex generation was highly dependent on the location of the blue-detuned potential, on its physical geometry, and on the amplitude of modulation. The specific mechanism of vortex creation is not yet fully clear, but counterflow or Kelvin-Helmholtz instabilities between the condensate part and the non-condensate component of the system is a possibility. Additionally, the observed oscillations in BEC size after beam modulation may be a limitation of this method if we are to use this in experimental studies of quantum turbulence that require observations of vortex dynamics and intervortex separations. Due to the size oscillation of the BEC, there will be instances that the vortex cores will be below the resolution limit of the imaging system.

7.3 Creation of a giant vortex

Using a newly developed technique, controlled generation of a multiply quantized vortex was implemented. This method involved the translation of a repulsive potential along a spiral trajectory within the BEC. This leads to a buildup of phase and quantized flow in the condensate. When the potentials ends up at the center of the BEC, it serves as a pinning potential for the created multiply quantized flow. The circulation number of the giant vortex is dependent on the translation speed of the repulsive potential. This technique could prove useful in phase slippage studies in BECs and those involving de-

cays of giant flows in superfluids. This method can also be applied to persistent current studies that require varying amounts of vorticity. Additionally, the instability of the multiply quantized vortex in the absence of a pinning potential can be utilized as a method to launch singly quantized vortices of the same circulation sign within the BEC.

7.4 Vortex tweezers: Creation and manipulation of vortices

Using a pair of repulsive potentials, two singly quantized vortices were repeatably generated and pinned in a highly oblate BEC. After their creation, manipulation of vortices was demonstrated by moving them within the condensate. This was accomplished by simply translating the repulsive potentials across the BEC towards the desired position for the vortex. This method paves the way for creating or engineering more complex vortex arrangements or patterns in a BEC in a repeatable manner.

As a final note, the experimental results that were mentioned above and discussed in Chapters 3-6 represent the different and broad experimental techniques and capabilities that have been newly developed to generate quantized vortices in highly oblate Bose-Einstein condensates: from generating seemingly random and disordered vortex configurations to controlled, deterministic, and repeatable creation of singly quantized vortices. These new techniques will prove beneficial in studies of vortex dynamics and interactions in highly oblate superfluid systems.

As was stated in this work, the dynamics of vortices in these systems are expected to be different from the typical vortex experiments in BECs because of the tight confinement in one direction of the system. This inhibits vortex twisting and bending and

interacting with one another as strongly as in 3D, and the motion and interaction of the vortices are limited to essentially a single plane. The capability to create disordered arrangements of vortices of either same or opposite circulations will be useful in two-dimensional studies of quantum turbulence. The novel method of creating multiply quantized vortices can be applied to systematic experimental studies of the decay of giant superflows in 2D. The ability to repeatably create and position singly quantized vortices of both circulation directions in a BEC is an initial step in devising more complex methods of engineering arbitrary vortex configurations. Essentially, the methods that were introduced in this dissertation will help in understanding two-dimensional dynamics of quantized vortices in atomic BECs by providing experimental tools that can be directly used or built upon to realize systematic experimental studies of this interesting area of superfluidity.

REFERENCES

[1] M. H. Anderson, *et al.*, "Observation of Bose-Einstein Condensation in a Dilute Atomic Vapor," *Science,* vol. 269, pp. 198-201, July 14, 1995 1995.

[2] C. C. Bradley, *et al.*, "Evidence of Bose-Einstein Condensation in an Atomic Gas with Attractive Interactions," *Physical Review Letters,* vol. 75, pp. 1687-1690, 1995.

[3] K. B. Davis, *et al.*, "Bose-Einstein Condensation in a Gas of Sodium Atoms," *Physical Review Letters,* vol. 75, pp. 3969-3973, 1995.

[4] B. Anderson, "Resource Article: Experiments with Vortices in Superfluid Atomic Gases," *Journal of Low Temperature Physics,* vol. 161, pp. 574-602, 2010.

[5] S. Stock, *et al.*, "Observation of Phase Defects in Quasi-Two-Dimensional Bose-Einstein Condensates," *Physical Review Letters,* vol. 95, p. 190403, 2005.

[6] Z. Hadzibabic, *et al.*, "Berezinskii-Kosterlitz-Thouless crossover in a trapped atomic gas," *Nature,* vol. 441, pp. 1118-1121, 2006.

[7] Z. Hadzibabic, *et al.*, "The trapped two-dimensional Bose gas: from Bose-Einstein condensation to Berezinskii-Kosterlitz-Thouless physics," *New Journal of Physics,* vol. 10, p. 045006, 2008.

[8] V. Schweikhard, *et al.*, "Vortex Proliferation in the Berezinskii-Kosterlitz-Thouless Regime on a Two-Dimensional Lattice of Bose-Einstein Condensates," *Physical Review Letters,* vol. 99, p. 030401, 2007.

[9] P. Cladé, *et al.*, "Observation of a 2D Bose Gas: From Thermal to Quasicondensate to Superfluid," *Physical Review Letters,* vol. 102, p. 170401, 2009.

[10] T. W. Neely, *et al.*, "Observation of Vortex Dipoles in an Oblate Bose-Einstein Condensate," *Physical Review Letters,* vol. 104, p. 160401, 2010.

[11] T. W. Neely, *et al.*, "Characteristics of Two-Dimensional Quantum Turbulence in a Compressible Superfluid," *ArXiv e-prints,* April 2012.

[12] S. J. Rooney, *et al.*, "Suppression of Kelvon-induced decay of quantized vortices in oblate Bose-Einstein condensates," *Physical Review A,* vol. 84, 2011.

[13] P. Rosenbusch, *et al.*, "Dynamics of a Single Vortex Line in a Bose-Einstein Condensate," *Physical Review Letters,* vol. 89, p. 200403, 2002.

[14] V. Bretin, *et al.*, "Dynamics of a single vortex line in a Bose-Einstein condensate," *Journal of Optics B: Quantum and Semiclassical Optics,* vol. 5, p. S23, 2003.

[15] V. Bretin, *et al.*, "Quadrupole Oscillation of a Single-Vortex Bose-Einstein Condensate: Evidence for Kelvin Modes," *Physical Review Letters,* vol. 90, p. 100403, 2003.

[16] T. W. Neely, "Formation, Dynamics, and Decay of Quantized Vortices in Bose-Einstein Condensates: Elements of Quantum Turbulence," PhD, College of Optical Sciences, University of Arizona, 2010.

[17] C. J. Pethick and H. Smith, *Bose-Einstein Condensation in Dilute Gases*. Cambridge: Cambridge University Press, 2002.

[18] P. G. Kevrekidis, *et al.*, Eds., *Emergent Nonlinear Phenomena in Bose-Einstein Condensates: Theory and Experiment* (Springer Series on Atomic, Optical, and Plasma Physics 45). Berlin: Springer-Verlag, 2008.

[19] L. Pitaevskii and S. Stringari, *Bose-Einstein Condensation*. Oxford: Oxford University Press, 2003.

[20] D. R. Scherer, "Vortex Formation by Merging and Interference of Multiple Trapped Bose-Einstein Condensates," PhD, College of Optical Sciences, University of Arizona, 2007.

[21] C. N. Weiler, "Spontaneous Formation of Quantized Vortices in Bose-Einstein Condensates," PhD, College of Optical Sciences, University of Arizona, 2008.

[22] W. Petrich, *et al.*, "Behavior of atoms in a compressed magneto-optical trap," *J. Opt. Soc. Am. B,* vol. 11, pp. 1332-1335, 1994.

[23] H. J. Metcalf and P. van der Straten, *Laser Cooling and Trapping*. New York: Springer-Verlag, 1999.

[24] V. Bagnato and D. Kleppner, "Bose-Einstein condensation in low-dimensional traps," *Physical Review A,* vol. 44, pp. 7439-7441, Dec 1 1991.

[25] K. W. Madison, *et al.*, "Vortex Formation in a Stirred Bose-Einstein Condensate," *Physical Review Letters,* vol. 84, pp. 806-809, 2000.

[26] J. R. Abo-Shaeer, *et al.*, "Observation of Vortex Lattices in Bose-Einstein Condensates," *Science,* vol. 292, pp. 476-479, April 20, 2001 2001.

[27] C. Raman, *et al.*, "Vortex Nucleation in a Stirred Bose-Einstein Condensate," *Physical Review Letters,* vol. 87, 2001.

[28] J. R. Abo-Shaeer, *et al.*, "Formation and Decay of Vortex Lattices in Bose-Einstein Condensates at Finite Temperatures," *Physical Review Letters,* vol. 88, p. 070409, 2002.

[29] K. W. Madison, *et al.*, "Stationary States of a Rotating Bose-Einstein Condensate: Routes to Vortex Nucleation," *Physical Review Letters,* vol. 86, pp. 4443-4446, 2001.

[30] P. C. Haljan, *et al.*, "Driving Bose-Einstein-Condensate Vorticity with a Rotating Normal Cloud," *Physical Review Letters,* vol. 87, p. 210403, 2001.

[31] P. Engels, *et al.*, "Observation of Long-Lived Vortex Aggregates in Rapidly Rotating Bose-Einstein Condensates," *Physical Review Letters,* vol. 90, p. 170405, 2003.

[32] E. Hodby, *et al.*, "Vortex Nucleation in Bose-Einstein Condensates in an Oblate, Purely Magnetic Potential," *Physical Review Letters,* vol. 88, p. 010405, 2001.

[33] D. L. Feder, *et al.*, "Nucleation of vortex arrays in rotating anisotropic Bose-Einstein condensates," *Physical Review A,* vol. 61, 1999.

[34] D. L. Feder, *et al.*, "Anomalous Modes Drive Vortex Dynamics in Confined Bose-Einstein Condensates," *Physical Review Letters,* vol. 86, pp. 564-567, 2001.

[35] A. A. Penckwitt, *et al.*, "Nucleation, Growth, and Stabilization of Bose-Einstein Condensate Vortex Lattices," *Physical Review Letters,* vol. 89, p. 260402, 2002.

[36] E. Lundh, *et al.*, "Vortex nucleation in Bose-Einstein condensates in time-dependent traps," *Physical Review A,* vol. 67, p. 063604, 2003.

[37] M. Tsubota, *et al.*, "Vortex lattice formation in a rotating Bose-Einstein condensate," *Physical Review A,* vol. 65, p. 023603, 2002.

[38] J. J. García-Ripoll and V. M. Pérez-García, "Vortex bending and tightly packed vortex lattices in Bose-Einstein condensates," *Physical Review A,* vol. 64, p. 053611, 2001.

[39] J. J. García-Ripoll and V. M. Pérez-García, "Vortex nucleation and hysteresis phenomena in rotating Bose-Einstein condensates," *Physical Review A,* vol. 63, p. 041603, 2001.

[40] A. Aftalion and T. Riviere, "Vortex energy and vortex bending for a rotating Bose-Einstein condensate," *Physical Review A,* vol. 64, p. 043611, 2001.

[41] A. Aftalion and R. L. Jerrard, "Shape of vortices for a rotating Bose-Einstein condensate," *Physical Review A,* vol. 66, p. 023611, 2002.

[42] N. L. Smith, *et al.*, "Experimental Observation of the Tilting Mode of an Array of Vortices in a Dilute Bose-Einstein Condensate," *Physical Review Letters,* vol. 93, p. 080406, 2004.

[43] N. Parker and C. Adams, "Emergence and Decay of Turbulence in Stirred Atomic Bose-Einstein Condensates," *Physical Review Letters,* vol. 95, 2005.

[44] N. G. Parker and C. S. Adams, "Response of an atomic Bose-Einstein condensate to a rotating elliptical trap," *Journal of Physics B: Atomic, Molecular and Optical Physics,* vol. 39, p. 43, 2006.

[45] T. M. Wright, *et al.*, "Dynamical thermalization and vortex formation in stirred two-dimensional Bose-Einstein condensates," *Physical Review A,* vol. 78, p. 063601, 2008.

[46] A. S. Bradley and B. P. Anderson, "Energy spectra of vortex distributions in two-dimensional quantum turbulence," *ArXiv e-prints,* April 2012.

[47] J. Arlt, *et al.*, "Bose-Einstein condensation in a rotating anisotropic TOP trap," *Journal of Physics B: Atomic, Molecular and Optical Physics,* vol. 32, p. 5861, 1999.

[48] K. W. Madison, *et al.*, "Vortices in a stirred Bose-Einstein condensate," *Journal of Modern Optics,* vol. 47, pp. 2715-2723, 2000/11/01 2000.

[49] S. Sinha and Y. Castin, "Dynamic Instability of a Rotating Bose-Einstein Condensate," *Physical Review Letters,* vol. 87, p. 190402, 2001.

[50] A. Recati, *et al.*, "Overcritical Rotation of a Trapped Bose-Einstein Condensate," *Physical Review Letters,* vol. 86, pp. 377-380, 2001.

[51] D. S. Jin, *et al.*, "Temperature-Dependent Damping and Frequency Shifts in Collective Excitations of a Dilute Bose-Einstein Condensate," *Physical Review Letters,* vol. 78, pp. 764-767, 1997.

[52] D. M. Stamper-Kurn, *et al.*, "Collisionless and Hydrodynamic Excitations of a Bose-Einstein Condensate," *Physical Review Letters,* vol. 81, pp. 500-503, 1998.

[53] A. Fetter, "Rotating trapped Bose-Einstein condensates," *Laser Physics,* vol. 18, pp. 1-11, 2008.

[54] A. L. Fetter, "Vortices and Dynamics in Trapped Bose-Einstein Condensates," *Journal of Low Temperature Physics,* vol. 161, pp. 445-459, 2010.

[55] A. L. Fetter and A. A. Svidzinsky, "Vortices in a trapped dilute Bose-Einstein condensate," *Journal of Physics: Condensed Matter,* vol. 13, 2001.

[56] D. Dagnino, *et al.*, "Vortex nucleation as a case study of symmetry breaking in quantum systems," *Nat Phys,* vol. 5, pp. 431-437, 2009.

[57] M. Ueda and T. Nakajima, "Nambu-Goldstone mode in a rotating dilute Bose-Einstein condensate," *Physical Review A,* vol. 73, p. 043603, 2006.

[58] T. K. Ghosh, "Vortex formation in a fast rotating Bose-Einstein condensate," *Physical Review A,* vol. 69, p. 043606, 2004.

[59] P. Rosenbusch, *et al.*, "Critical Rotation of a Harmonically Trapped Bose Gas," *Physical Review Letters,* vol. 88, 2002.

[60] D. S. Rokhsar, "Vortex Stability and Persistent Currents in Trapped Bose Gases," *Physical Review Letters,* vol. 79, pp. 2164-2167, 1997.

[61] A. L. Fetter, "Vortex Stability in a Trapped Bose Condensate," *Journal of Low Temperature Physics,* vol. 113, pp. 189-194, 1998.

[62] A. A. Svidzinsky and A. L. Fetter, "Stability of a Vortex in a Trapped Bose-Einstein Condensate," *Physical Review Letters,* vol. 84, pp. 5919-5923, 2000.

[63] B. Jackson, *et al.*, "Finite-temperature vortex dynamics in Bose-Einstein condensates," *Physical Review A,* vol. 79, 2009.

[64] T. M. Wright, *et al.*, "Finite-temperature dynamics of a single vortex in a Bose-Einstein condensate: Equilibrium precession and rotational symmetry breaking," *Physical Review A,* vol. 80, p. 053624, 2009.

[65] P. O. Fedichev and G. V. Shlyapnikov, "Dissipative dynamics of a vortex state in a trapped Bose-condensed gas," *Physical Review A,* vol. 60, pp. R1779-R1782, 1999.

[66] I. Coddington, *et al.*, "Experimental studies of equilibrium vortex properties in a Bose-condensed gas," *Physical Review A,* vol. 70, p. 063607, 2004.

[67] R. Blaauwgeers, *et al.*, "Shear Flow and Kelvin-Helmholtz Instability in Superfluids," *Physical Review Letters,* vol. 89, p. 155301, 2002.

[68] G. Volovik, "On the Kelvin-Helmholtz instability in superfluids," *JETP Letters,* vol. 75, pp. 418-422, 2002.

[69] E. A. L. Henn, *et al.*, "Generation of Vortices and Observation of Quantum Turbulence in an Oscillating Bose-Einstein Condensate," *Journal of Low Temperature Physics,* vol. 158, pp. 435-442, 2009.

[70] E. Henn, *et al.*, "Observation of vortex formation in an oscillating trapped Bose-Einstein condensate," *Physical Review A,* vol. 79, 2009.

[71] L. Skrbek, "Counterflow Turbulence in He II and Its Decay

Vortices and Turbulence at Very Low Temperatures." vol. 501, C. F. Barenghi and Y. A. Sergeev, Eds.: Springer Vienna, 2008, pp. 91-137.

[72] H. Adachi and M. Tsubota, "Numerical Studies of Counterflow Turbulence," *Journal of Low Temperature Physics,* vol. 158, pp. 422-427, 2010.

[73] M. Sciacca, *et al.*, "Saturation of decaying counterflow turbulence in helium II," *Physical Review B,* vol. 82, p. 134531, 2010.

[74] U. R. Fischer and G. Baym, "Vortex States of Rapidly Rotating Dilute Bose-Einstein Condensates," *Physical Review Letters,* vol. 90, p. 140402, 2003.

[75] E. Lundh, "Multiply quantized vortices in trapped Bose-Einstein condensates," *Physical Review A,* vol. 65, 2002.

[76] K. Kasamatsu, *et al.*, "Giant hole and circular superflow in a fast rotating Bose-Einstein condensate," *Physical Review A,* vol. 66, 2002.

[77] M. Correggi, *et al.*, "The Transition to a Giant Vortex Phase in a Fast Rotating BEC." Vienna: The Erwin Schrodinger International Institute for Mathematical Physics, 2010.

[78] M. Correggi, *et al.*, "Rotating superfluids in anharmonic traps: From vortex lattices to giant vortices," *Physical Review A,* vol. 84, p. 053614, 2011.

[79] R. J. Donnely, *Quantized vortices in helium II*. Cambridge: Cambridge University Press, 1991.

[80] A. E. Leanhardt, *et al.*, "Imprinting Vortices in a Bose-Einstein Condensate using Topological Phases," *Physical Review Letters,* vol. 89, p. 190403, 2002.

[81] M. Kumakura, *et al.*, "Topological creation of a multiply charged quantized vortex in the Rb Bose-Einstein condensate," *Laser Physics,* vol. 16, pp. 371-375, 2006.

[82] Y. Kawaguchi and T. Ohmi, "Splitting instability of a multiply charged vortex in a Bose-Einstein condensate," *Physical Review A,* vol. 70, p. 043610, 2004.

[83] T. Isoshima, *et al.*, "Spontaneous Splitting of a Quadruply Charged Vortex," *Physical Review Letters,* vol. 99, p. 200403, 2007.

[84] M. Okano, *et al.*, "Splitting of a Quadruply Quantized Vortex in the Rb Bose-Einstein Condensate," *Journal of Low Temperature Physics,* vol. 148, pp. 447-451, 2007.

[85] M. F. Andersen, *et al.*, "Quantized Rotation of Atoms from Photons with Orbital Angular Momentum," *Physical Review Letters,* vol. 97, p. 170406, 2006.

[86] C. Ryu, *et al.*, "Observation of Persistent Flow of a Bose-Einstein Condensate in a Toroidal Trap," *Physical Review Letters,* vol. 99, 2007.

[87] A. Ramanathan, *et al.*, "Superflow in a Toroidal Bose-Einstein Condensate: An Atom Circuit with a Tunable Weak Link," *Physical Review Letters,* vol. 106, 2011.

[88] J. F. S. Brachmann, *et al.*, "Inducing vortices in a Bose-Einstein condensate using holographically produced light beams," *Opt. Express,* vol. 19, pp. 12984-12991, 2011.

[89] M. Möttönen, *et al.*, "Vortex Pump for Dilute Bose-Einstein Condensates," *Physical Review Letters,* vol. 99, 2007.

[90] P. Kuopanportti and M. Möttönen, "Stabilization and Pumping of Giant Vortices in Dilute Bose–Einstein Condensates," *Journal of Low Temperature Physics,* vol. 161, pp. 561-573, 2010.

[91] J. J. García-Ripoll and V. M. Pérez-García, "Stability of vortices in inhomogeneous Bose condensates subject to rotation: A three-dimensional analysis," *Physical Review A,* vol. 60, pp. 4864-4874, 1999.

[92] Y. Shin, *et al.*, "Dynamical Instability of a Doubly Quantized Vortex in a Bose-Einstein Condensate," *Physical Review Letters,* vol. 93, p. 160406, 2004.

[93] K. Tomasz, *et al.*, "Decay of multiply charged vortices at nonzero temperatures," *Journal of Physics B: Atomic, Molecular and Optical Physics,* vol. 42, p. 095301, 2009.

[94] P. W. Anderson, "Considerations on the Flow of Superfluid Helium," *Reviews of Modern Physics,* vol. 38, pp. 298-310, 1966.

[95] D. A. Butts and D. S. Rokhsar, "Predicted signatures of rotating Bose-Einstein condensates," *Nature,* vol. 397, pp. 327-329, Jan 28 1999.

[96] T. Simula*, et al.*, "Stability of multiquantum vortices in dilute Bose-Einstein condensates," *Physical Review A,* vol. 65, 2002.

[97] Y. Castin and R. Dum, "Bose-Einstein condensates with vortices in rotating traps," *The European Physical Journal D,* vol. 7, pp. 399-412, 1999.

[98] P. Capuzzi and D. M. Jezek, "Stationary arrays of vortices in Bose-Einstein condensates confined by a toroidal trap," *Journal of Physics B: Atomic, Molecular and Optical Physics,* vol. 42, p. 145301, 2009.

[99] B. P. Anderson*, et al.*, "Watching Dark Solitons Decay into Vortex Rings in a Bose-Einstein Condensate," *Physical Review Letters,* vol. 86, pp. 2926-2929, 2001.

[100] S. Komineas and N. Papanicolaou, "Solitons, solitonic vortices, and vortex rings in a confined Bose-Einstein condensate," *Physical Review A,* vol. 68, p. 043617, 2003.

[101] M. C. Davis*, et al.*, "Manipulation of vortices by localized impurities in Bose-Einstein condensates," *Physical Review A,* vol. 80, p. 023604, 2009.